University of Massachusetts Medical School

eScholarship@UMMS

Open Access Articles | Open Access Publications by UMMS Authors

2018-11-06

Genetic Models Reveal cis and trans Immune-Regulatory Activities for lincRNA-Cox2

Roland Elling
University of Massachusetts Medical School

Et al.

Let us know how access to this document benefits you.

Follow this and additional works at: https://escholarship.umassmed.edu/oapubs

 Part of the Genetic Phenomena Commons, Genetics and Genomics Commons, Immunity Commons, and the Nucleic Acids, Nucleotides, and Nucleosides Commons

Repository Citation

Elling R, Jiang Z, Agarwal S, Motwani M, Chan J, Sharma S, Fitzgerald KA, Carpenter S. (2018). Genetic Models Reveal cis and trans Immune-Regulatory Activities for lincRNA-Cox2. Open Access Articles. https://doi.org/10.1016/j.celrep.2018.10.027. Retrieved from https://escholarship.umassmed.edu/oapubs/3664

Creative Commons License

This work is licensed under a Creative Commons Attribution-Noncommercial-No Derivative Works 4.0 License.
This material is brought to you by eScholarship@UMMS. It has been accepted for inclusion in Open Access Articles by an authorized administrator of eScholarship@UMMS. For more information, please contact Lisa.Palmer@umassmed.edu.

Article

Cell Reports

Genetic Models Reveal *cis* and *trans* Immune-Regulatory Activities for lincRNA-Cox2

Graphical Abstract

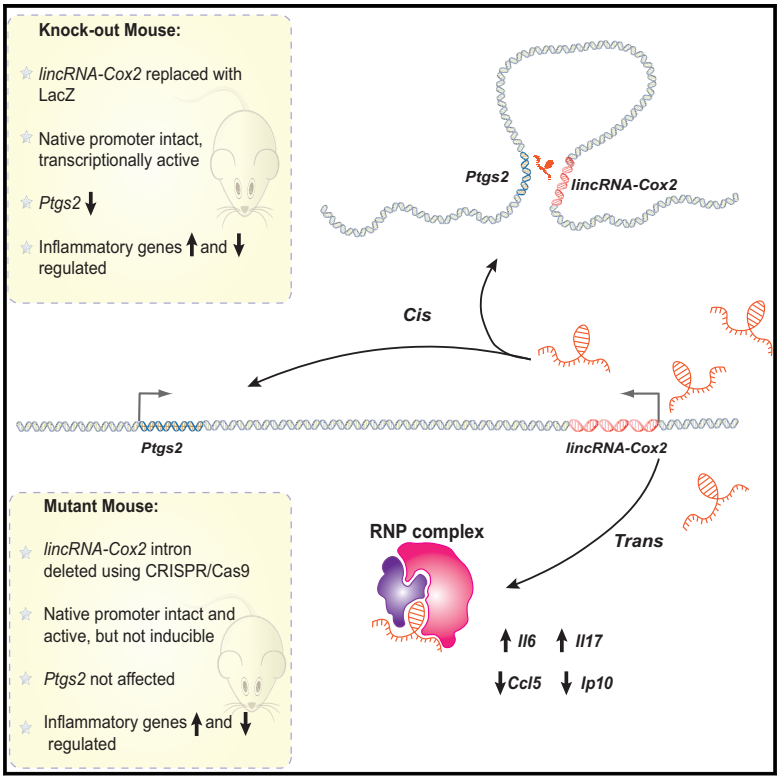

Highlights

- Study of *lincRNA-Cox2 in vivo* using recently generated KO and splicing mutant mice
- *lincRNA-Cox2* functions through an enhancer RNA mechanism to regulate *Ptgs2* levels
- *lincRNA-Cox2* has a *trans* regulatory role controlling many innate immune genes
- The lincRNA locus simultaneously regulates the expression of local and distant genes

Authors

Roland Elling, Elektra K. Robinson, Barbara Shapleigh, ..., John L. Rinn, Katherine A. Fitzgerald, Susan Carpenter

Correspondence

sucarpen@ucsc.edu

In Brief

Elling et al. utilize a number of *lincRNA-Cox2* genetic models to show that *lincRNA-Cox2* can regulate its neighboring gene *Ptgs2* (*Cox2*) through an enhancer RNA mechanism. They generate a *lincRNA-Cox2* splicing-deficient mouse and confirm that *lincRNA-Cox2* functions in *trans* to regulate immune genes following LPS-induced endotoxic shock.

Elling et al., 2018, Cell Reports *25*, 1511–1524
November 6, 2018
https://doi.org/10.1016/j.celrep.2018.10.027

CellPress

Cell Reports
Article

OPEN ACCESS
CellPress

Genetic Models Reveal *cis* and *trans* Immune-Regulatory Activities for lincRNA-Cox2

Roland Elling,[1,2,10] Elektra K. Robinson,[3,10] Barbara Shapleigh,[3] Stephen C. Liapis,[4] Sergio Covarrubias,[3] Sol Katzman,[5] Abigail F. Groff,[4] Zhaozhao Jiang,[1] Shiuli Agarwal,[1] Mona Motwani,[1] Jennie Chan,[1] Shruti Sharma,[1] Elizabeth J. Hennessy,[6] Garret A. FitzGerald,[6] Michael T. McManus,[7,8] John L. Rinn,[4,9] Katherine A. Fitzgerald,[1,11] and Susan Carpenter[3,11,12,*]

[1]Program in Innate Immunity, Department of Medicine, University of Massachusetts Medical School, Worcester, MA, USA
[2]Center for Pediatrics, Department of General Pediatrics, University of Freiburg, Freiburg, Germany
[3]Department of Molecular, Cell and Developmental Biology, University of California, Santa Cruz, Santa Cruz, CA, USA
[4]Harvard Stem Cell and Regenerative Biology Department, Harvard University, Cambridge, MA 02138, USA
[5]Center for Biomolecular Science and Engineering, University of California, Santa Cruz, Santa Cruz, CA, USA
[6]Department of Systems Pharmacology and Translational Therapeutics, Perelman School of Medicine, University of Pennsylvania, 3400 Civic Center Boulevard, Smilow, Philadelphia, PA 19104, USA
[7]Department of Microbiology and Immunology, University of California, San Francisco, San Francisco, CA, USA
[8]UCSF Diabetes Center, University of California, San Francisco, San Francisco, CA, USA
[9]Department of Biochemistry, BioFrontiers, University of Colorado Boulder, Boulder, CO 80301, USA
[10]These authors contributed equally
[11]Senior author
[12]Lead Contact
*Correspondence: sucarpen@ucsc.edu
https://doi.org/10.1016/j.celrep.2018.10.027

SUMMARY

An inducible gene expression program is a hallmark of the host inflammatory response. Recently, long intergenic non-coding RNAs (lincRNAs) have been shown to regulate the magnitude, duration, and resolution of these responses. Among these is *lincRNA-Cox2*, a dynamically regulated gene that broadly controls immune gene expression. To evaluate the *in vivo* functions of this lincRNA, we characterized multiple models of *lincRNA-Cox2*-deficient mice. *LincRNA-Cox2*-deficient macrophages and murine tissues had altered expression of inflammatory genes. Transcriptomic studies from various tissues revealed that deletion of the *lincRNA-Cox2* locus also strongly impaired the basal and inducible expression of the neighboring gene prostaglandin-endoperoxide synthase (*Ptgs2*), encoding cyclooxygenase-2, a key enzyme in the prostaglandin biosynthesis pathway. By utilizing different genetic manipulations *in vitro* and *in vivo*, we found that *lincRNA-Cox2* functions through an enhancer RNA mechanism to regulate *Ptgs2*. More importantly, *lincRNA-Cox2* also functions in *trans*, independently of Ptgs2, to regulate critical innate immune genes *in vivo*.

INTRODUCTION

Activation of myeloid cells is associated with differential expression of immune genes involved in host defense, tissue repair, and resolution of inflammation. Toll-like receptors (Tlrs) are germline-encoded receptors critical for the activation of signaling pathways controlling immune response genes. Dysregulation of these pathways can lead to deleterious autoinflammatory conditions, which can contribute to autoimmunity or cancer (Gajewski et al., 2013; Gierut et al., 2010; Masters et al., 2009). Tight control of these inflammatory signaling cascades is required to prevent host damage and is achieved both transcriptionally and posttranscriptionally.

The majority of mammalian genomes are pervasively transcribed, producing thousands of noncoding RNAs (ENCODE Project Consortium, 2012). Interestingly, the expression of these noncoding genes is highly cell type-specific (Morris and Mattick, 2014), and their function remains largely unknown. Long intergenic noncoding RNAs (lincRNAs) are a subclass of long noncoding RNAs (lncRNAs) that form the largest class of RNA produced in the genome. The tremendous number of newly annotated lincRNAs and their low evolutionary conservation has led to debates about their functionality (Bassett et al., 2014). However, the number of characterized lincRNAs is growing, and this class of gene has been shown to control various biological processes, including somatic tissue differentiation (Kretz et al., 2013), X chromosome inactivation (Carmona et al., 2018; Engreitz et al., 2013; Jégu et al., 2017), and organ development (Anderson et al., 2016).

LincRNAs function to control gene expression either in *cis*, where they influence the expression and/or chromatin state of neighboring genes, or in *trans*, where the lincRNA leaves the site of transcription and affects genes on different chromosomes (Kopp and Mendell, 2018; Liang et al., 2018; Neumann et al., 2018). These *trans*-acting lincRNAs, such as FOXF1 adjacent non-coding developmental regulatory RNA (FENDRR), long-intergenic non-coding-erythroid prosurvival (linc-EPS), and Nettoie Salmonella pas Theiler's (NeST), can function to regulate

This is an open access article under the CC BY-NC-ND license (http://creativecommons.org/licenses/by-nc-nd/4.0/).

chromatin states (Atianand et al., 2016; Gomez et al., 2013; Grote et al., 2013; Sauvageau et al., 2013), influence nuclear structure and organization (Rinn and Guttman, 2014), or interact with and regulate the behavior of proteins and/or other RNA molecules (Covarrubias et al., 2017; Kawasaki et al., 2018; Lee et al., 2016; Wang et al., 2017).

lincRNAs have recently been shown to regulate the development and function of immune cells (Kotzin et al., 2016; Wang et al., 2014, 2017). Previous work from our lab and others defined an immune-inducible lincRNA, *lincRNA-Cox2* (synonym Ptgs2os2) with broad *trans*-regulatory activity on inflammatory responses (Carpenter et al., 2013; Covarrubias et al., 2017; Hu et al., 2016; Tong et al., 2016; Xue et al., 2018). In macrophages, where this lincRNA was highly induced upon inflammatory activation, *lincRNA-Cox2* functioned to activate and repress distinct classes of innate immune genes (Carpenter et al., 2013). However, like most lincRNAs and protein-coding genes, the *cis*- and *trans*-regulatory elements encoded within the locus remain unstudied *in vivo*. Most recently, some lincRNAs have been discovered to have the ability to function both in *cis* and in *trans* (Carmona et al., 2018; Li et al., 2012; Yin et al., 2015).

Here we created a combination of different genetic deletion models to study the role of the *lincRNA-Cox2* locus in macrophages and in murine models *in vivo*. Consistent with prior work, we found that *lincRNA-Cox2*-deficient macrophages had altered expression of numerous inflammatory genes (Carpenter et al., 2013; Covarrubias et al., 2017). In addition, we observed a profound *cis* function for *lincRNA-Cox2*: *lincRNA-Cox2*-deficient mice had severely reduced expression of the neighboring gene *Ptgs2*, a gene that encodes for cyclooxygenase-2 (Cox2), a central enzyme of the prostaglandin biosynthesis pathway, across several tissues. This finding provides evidence for a previously unrecognized *cis* function for *lincRNA-Cox2*. We have data that support *lincRNA-Cox2* functioning through an RNA-mediated mechanism as an enhancer RNA (eRNA) to regulate *Ptgs2* expression. Crossing our *lincRNA-Cox2*-deficient mice to wild-derived mice (MOLF) that have a distinct genetic background provides critical evidence that *lincRNA-Cox2* indeed functions on the same chromosome to regulate *Ptgs2* expression levels.

Finally, to distinguish the *cis*-regulatory element from the *trans* activity of the RNA transcript, we generated a "mutant" mouse model that retained the exonic sequences of the lincRNA but lacked the intron and splicing capabilities. This resulted in a mouse with a low basal expression level of *lincRNA-Cox2,* but the transcript is no longer inducible following inflammatory stimulation. In the mutant mouse, *Ptgs2* expression is comparable with wild-type mice as the eRNA activity of the lincRNA-Cox2 locus is maintained. Using a conventional *in vivo* lipopolysaccharide (LPS) shock model, we identify an additional role for the *lincRNA-Cox2* transcript in the *trans* regulation of a subset of immune genes as well as an organ-specific role independent of *Ptgs2* biology. Collectively, these observations reveal a bimodal action of gene regulation by the *lincRNA-Cox2* transcript: a *trans*-regulatory function controlling immune genes such as cytokines globally and a separate enhancer function acting to regulate prostaglandin biosynthesis via Ptgs2 (Cox2). Thus, *lincRNA-Cox2* represents a regulator of the *Ptgs2* pathway as well as an important mediator of immunity beyond the prostaglandin pathway.

RESULTS

Genetic Deletion of *lincRNA-Cox2* Alters Immune Gene Expression in Macrophages

LincRNA-Cox2 is encoded on chromosome 1 and transcribed from the negative strand. The mature sequence has 2 exons and is 1.7 kb long. Its nearest protein coding gene, prostaglandin-endoperoxide synthase 2 (Ptgs2 or Cox2), is ~50 kb upstream and transcribed on the positive strand (Figure 1A). A *lincRNA-Cox2* knockout (KO) mouse was generated by removing the entire genomic locus (5.9 kB), except for the promoter, and replacing it with a LacZ reporter cassette (Sauvageau et al., 2013; Figure 1B). KO mice were born at expected Mendelian frequencies with no obvious developmental abnormalities (Sauvageau et al., 2013). We and others have previously published that *lincRNA-Cox2* acts to positively and negatively regulate the expression of distinct classes of innate immune genes (Carpenter et al., 2013; Covarrubias et al., 2017; Hu et al., 2016; Tong et al., 2016; Xue et al., 2018). In those studies, short hairpin RNA (shRNA)-based knockdown of *lincRNA-Cox2* reduced the levels of pro-inflammatory cytokines like *Interleukin-6* (*Il6*) in bone-marrow derived macrophages (BMDMs) activated with LPS, whereas a number of interferon-stimulated genes (ISGs) were expressed at higher levels. Here, using genetic approaches, we find that *lincRNA-Cox2*-deficient BMDMs (Figure 1C) produced less *Il6* (Figure 1D) and more *Chi3L* as well as *Ifl202b*, an ISG, following LPS (Tlr4) and R848 (Tlr7) stimulation (Figures 1E and 1F).

Ptgs2 Levels Are Reduced in *lincRNA-Cox2* KO Mice

The *lincRNA-Cox2* KO mouse was generated so that the locus remains transcriptionally active and LacZ staining can be used as a surrogate for *lincRNA-Cox2* expression (Sauvageau et al., 2013). Staining of several organs from these mice revealed the *in vivo* expression of *lincRNA-Cox2* in both the brain (dorsal cerebral cortex) and the lung under steady-state conditions (Figure 2A). Further, RNA sequencing (RNA-seq) from a variety of organs confirmed that *lincRNA-Cox2* was most highly expressed in the lung at steady state (Figure S1A). To identify the target genes of *lincRNA-Cox2* at steady state, we performed RNA-seq on whole lung tissue, comparing wild-type and *lincRNA-Cox2*-deficient mice. Using differential expression sequencing 2 (DESeq2) with a cut off of 2.5-fold and a p value of 0.05, 476 genes showed altered expression (273 were upregulated and 203 were downregulated) (Table S1). Among the most significantly downregulated genes was *Ptgs2* (Figure 2B, highlighted in red).

Next we wanted to investigate the *lincRNA-Cox2* locus at higher resolution and across different tissues to understand whether this effect was specific to *Ptgs2* or whether the genetic manipulation of the locus altered other neighboring genes. To that end, we compared the transcriptomes from WT and KO animal brains and lungs and generated *cis* region plots spanning a 1-Mb window in the vicinity of the *lincRNA-Cox2* locus. In both the lung and brain, which have high expression of lincRNA-Cox2

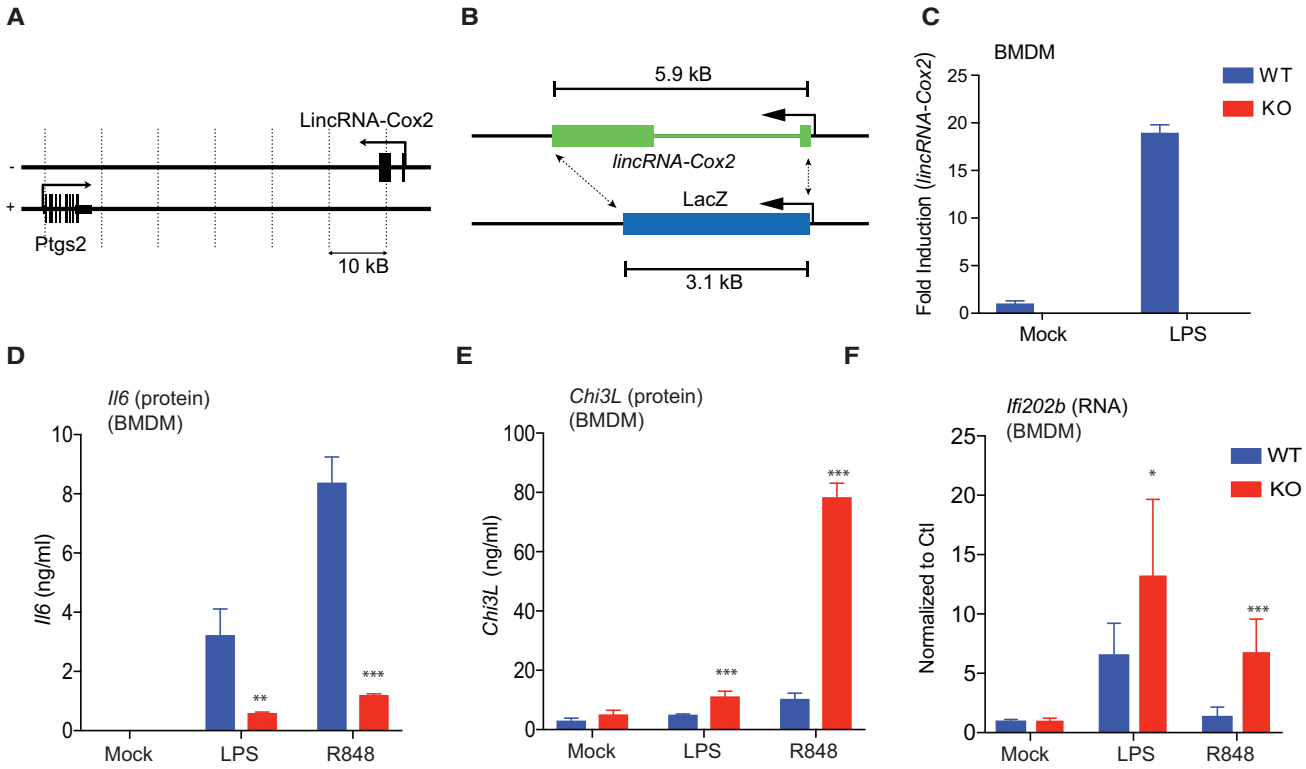

Figure 1. Characterization of the *lincRNA-Cox2* Knockout BMDMs

(A) Schematic showing that the *lincRNA-Cox2* locus is ~50 kb away from its closest protein-coding gene, *Ptgs2*.

(B) Schematic depicting the generation of the *lincRNA-Cox2* knockout mouse in which the locus has been replaced with a LacZ reporter construct.

(C) lincRNA-Cox2 expression levels were measured using qRT-PCR in wild-type (WT) or knockout (KO) macrophages treated with LPS for 6 hr.

(D and E) Bone marrow-derived macrophages (BMDMs) were treated with LPS for 24 hr; *Il6* (D) and *Chi3L* (E) levels were measured by ELISA.

(F) BMDMs were treated with LPS or R848, and *Ifi202b* levels were measured by qRT-PCR, normalized to the housekeeping gene *Gapdh*, and expressed as fold change over unstimulated cells.

Error bars represent standard deviation of biological triplicates. Student's t tests were performed using GraphPad Prism. Asterisks indicate statistically significant differences between mouse lines (*p ≥ 0.05, **p ≥ 0.01, ***p ≥ 0.005).

represented by LacZ staining in organs from KO mice (Figure 2A), the only gene affected in this region at steady state was *Ptgs2* (Figures S2A and S2B). To determine whether the *cis* effect on *Ptgs2* persisted after an inflammatory stimulus *in vivo*, a context in which the lincRNA transcript is highly induced, we measured the expression of *Ptgs2* in the lung, spleen, and liver following intraperitoneal (i.p.) injection of *E. coli* LPS (20 mg/kg) for 6 hr. In WT mice, *lincRNA-Cox2* and *Ptgs2* were inducible in the spleen and liver (Figures 2C–2G) following LPS treatment. *Ptgs2* levels were reduced in all tissues examined from *lincRNA-Cox2* KO mice following LPS challenge (Figures 2D–2H). LacZ expression remained comparable with *lincRNA-Cox2* expression in the tissues from KO mice following LPS treatment, confirming that the locus is actively transcribed (Figures S2C and S2D).

We also examined *Ptgs2* levels in BMDMs from the *lincRNA-Cox2* KO mice following stimulation with various Tlr ligands. In each case, the inducible transcriptional expression of *Ptgs2* was greatly reduced (Figure 2I). We confirmed this effect at the protein level in *lincRNA-Cox2*-deficient BMDMs by immunoblotting for Ptgs2 (Figure 2J). Ptgs2 is the central enzyme of the prostaglandin pathway catalyzing the conversion of arachidonic acid to prostaglandins (Ricciotti and FitzGerald, 2011). Consistent with the reduced expression of *Ptgs2* RNA and protein, there was reduced pro-inflammatory prostaglandin E2 (PGE2) production in *lincRNA-Cox2*-deficient cells as measured by mass spectrometry (Figure 2K). Together, all of these data indicate that the *lincRNA-Cox2* locus controls the expression of *Ptgs2* and, therefore, prostaglandin biosynthesis.

Rescue of Mature *lincRNA-Cox2* Fails to Restore Inducible *Ptgs2* Expression in Macrophages

LincRNA-Cox2 and *Ptgs2* show parallel inducible expression kinetics following Tlr activation. In prior work, we showed that knocking down the lincRNA transcript using shRNA had no effect on the expression of *Ptgs2* (Carpenter et al., 2013). This observation contrasts with the strong *cis* effect of the lincRNA locus observed in our KO model and could be consistent with a DNA-mediated enhancer effect, a mechanism that has previously been reported for other lincRNA loci (Engreitz et al., 2016; Groff et al., 2016; Joung et al., 2017; Paralkar et al., 2016). To gain more insight into the molecular basis for this *cis*

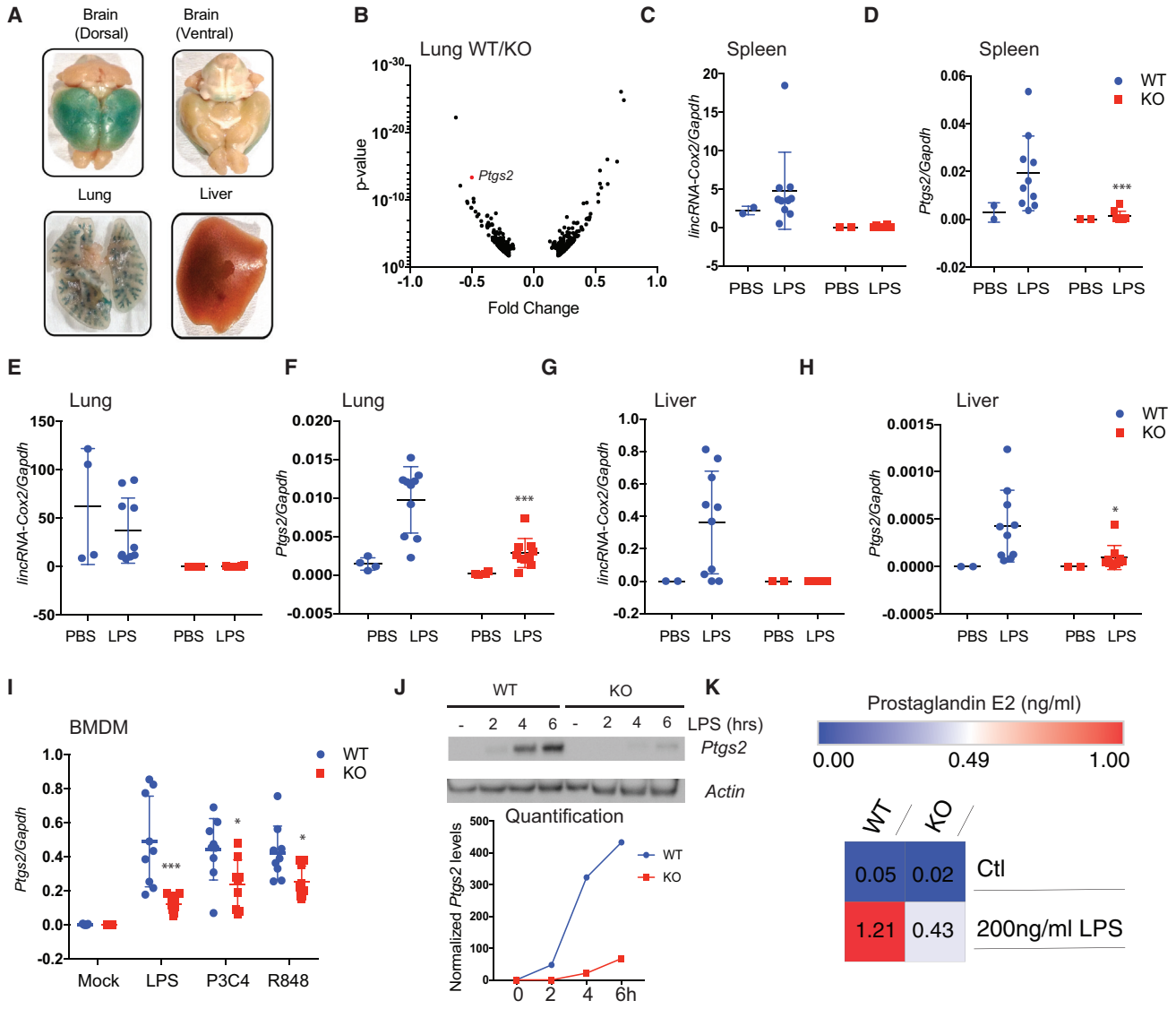

Figure 2. *lincRNA-Cox2* Expression in the Lung and Effects on *Ptgs2* in *cis*

(A) Brain, lung, and liver were stained for LacZ expression.

(B) RNA sequencing was performed on lung tissue, comparing WT and KO samples. The volcano plot represents the top upregulated and downregulated genes, comparing KO-WT using DESeq (cutoff of 1.5 log2 fold change in expression with $p > 0.05$). Ptgs2 is labeled in red.

(C–H) WT and *lincRNA-Cox2* KO mice were injected with LPS (20 mg/kg) for 6 hr, and spleens and lungs were extracted. The expression levels of *lincRNA-Cox2* (C, E, and G) and *Ptgs2* (D, F, and H) were tested by qRT-PCR and normalized to *Gapdh*. Each dot represents an individual animal. Error bars represent standard deviation of biological triplicates. Asterisks indicate statistically significant differences between mouse lines (Student's t test with $^{***}p \leq 0.05$). Student's t tests were performed using GraphPad Prism to obtain p values.

(I) BMDMs were stimulated with Tlr ligands for 6 hr, and Ptgs2 levels were measured by qPCR and normalized against Gapdh.

(J) BMDMs were stimulated with LPS for the indicted times, and *Ptgs2* levels were measured by western blot and quantified below.

(K) Phosphodiesterase (PDE) levels in WT and KO BMDMs was measured by mass spectrometry. The heatmap was generated by Morpheus (Broad Institute).

effect, we reconstituted *lincRNA-Cox2*-deficient primary BMDMs with the full-length spliced mature RNA transcript (Figure 3A) via plasmid electroporation. Despite restoration of *lincRNA-Cox2* to a level of expression comparable with that seen in wild-type (WT) cells, *Ptgs2* expression could not be rescued (Figure 3B). To control for possible effects mediated by knockin of the LacZ transgene, we also generated a BMDM line lacking *lincRNA-Cox2* using CRISPR/Cas9 to validate these findings. We designed guide RNAs to the 5′ and 3′ ends of the *lincRNA-Cox2* gene as outlined in Figure 3C, using two guide RNAs that remove the entire locus encoding the gene (while leaving the promoter intact). KO of *lincRNA-Cox2* was confirmed by qRT-PCR (Figure 3D). *Ptgs2* levels were also impaired in these Cas9-edited cells (Figure 3E). Again, reconstitution

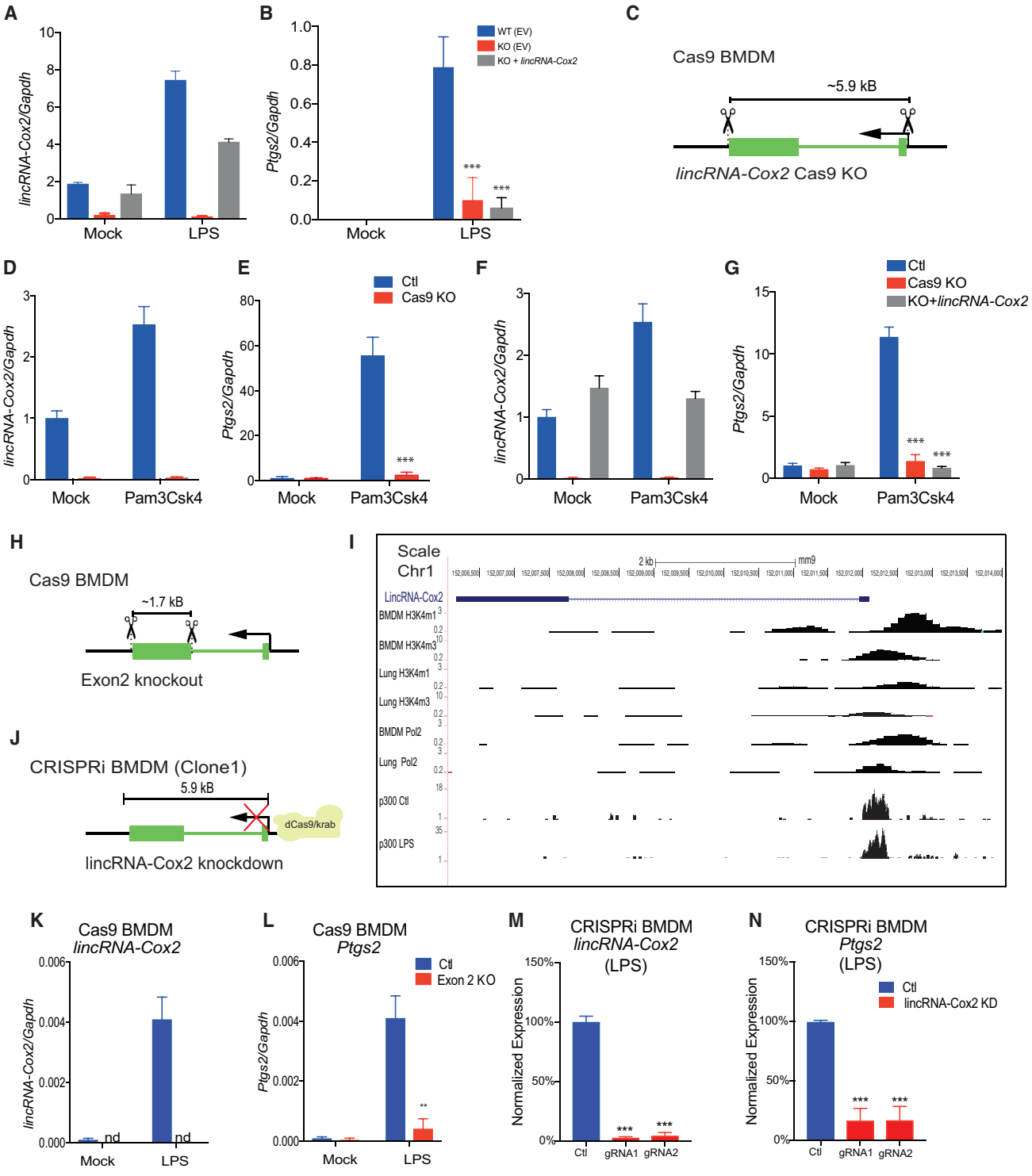

Figure 3. *lincRNA-Cox2* Acts as an eRNA to Control *Ptgs2*

(A) Primary BMDMs from the *lincRNA-Cox2* KO mice were reconstituted by plasmid electroporation with full-length *lincRNA-Cox2*. Expression of *lincRNA-Cox2* was confirmed by qRT-PCR.

(B) *Ptgs2* levels were determined by qRT-PCR in the *lincRNA-Cox2*-reconstituted cells. Data represent 2 combined biological replicates representative of 3 individual experiments.

(C) Schematic of the BMDM cell line using CRISPR/Cas9 to remove the *lincRNA-Cox2* locus.

(D and E) Expression of *lincRNA-Cox2* (D) and *Ptgs2* (E) was determined by qRT-PCR in the *lincRNA-Cox2* Cas9 KO BMDMs.

(legend continued on next page)

with the full-length *lincRNA-Cox2* transcript by lentiviral expression, which localized to both the nuclear and cytoplasmic compartments (Figures S3A and S3B), failed to rescue this phenotype (Figures 3F and 3G).

lincRNA-Cox2 Functions through an eRNA Mechanism to Regulate *Ptgs2*

Recently, it has been shown that non-coding RNA loci have the potential to harbor enhancer activities (Engreitz et al., 2016; Groff et al., 2016; Kim et al., 2015; Kotzin et al., 2016; Melo et al., 2013; Paralkar et al., 2016; Ørom et al., 2010). Because the effect of *lincRNA-Cox2* deficiency on *Ptgs2* levels was not rescued by ectopic expression, we speculated that the *lincRNA-Cox2* locus harbored a DNA enhancer element controlling *Ptgs2* expression. *LincRNA-Cox2* possesses two exons, with the majority of the sequence lying within exon 2. Using CRISPR/Cas9, we excised exon 2 from *lincRNA-Cox2* in BMDMs (Figure 3H) and confirmed this deletion by qRT-PCR (Figure 3K). *Ptgs2* was measured by qRT-PCR, and expression was markedly reduced in the exon 2 KO BMDMs, again suggesting that either the lincRNA transcript or a DNA enhancer element within exon 2 is required for the activity on *Ptgs2* (Figure 3L). These data confirm that there is no enhancer activity lying within exon 1, which remains intact in this model. To determine whether there are any enhancer marks present within exon 2 of lincRNA-Cox2, we studied chromatin immunoprecipitation sequencing (ChIP-seq) of histone marks associated with enhancers, including histone 3 lysine 4 (H3K4) mono-methylation, as well as p300 binding from the Mouse Encode project and from Lara-Astiaso et al. (2014) and Stamatoyannopoulos et al. (2012). We were surprised that there was no evidence of any enhancer within exon 2 of lincRNA-Cox2 and, instead, enhancer marks were identified upstream of the transcription start site of *lincRNA-Cox2* (Figure 3I; Figure S4). These data suggest that this locus might function instead as an eRNA in which transcription of *lincRNA-Cox2* functions to connect the enhancer region with the *Ptgs2* locus to drive expression of the protein. The enhancer region within the *lincRNA-Cox2* promoter remains intact in the KO mouse, and the locus is transcriptionally active, but there is a strong defect in *Ptgs2* levels. Only the *lincRNA-Cox2* transcript is absent in this model, and because there are no identifiable enhancer elements within this region, it suggests that specific transcription of the lincRNA-Cox2 sequence is driving this phenotype as an eRNA.

To test whether *lincRNA-Cox2* can function as an eRNA, we used CRISPR interference (CRISPRi) as outlined in Figure 3J to inhibit transcription of the locus. We successfully knocked down *lincRNA-Cox2* by over 95% using two independent guide RNAs in a clonal cell line (Figure 3M), and each led to a more than 95% decrease in *Ptgs2* expression, as assayed using qRT-PCR (Figure 3N). This result was replicated in a second CRISPRi BMDM cell line (Figures S5C and S5D). These data strongly indicate that it is locus-specific transcription of *lincRNA-Cox2* and not a DNA element within the exonic sequence of the gene that is critical to its function to control *Ptgs2* levels.

To determine whether *lincRNA-Cox2* regulates *Ptgs2* on the same chromosome, one final experiment was performed using mice with distinct genetic backgrounds. We took advantage of the wild-derived mouse strain MOLF, which is genetically distinct from the common laboratory C57/Bl6 mice. MOLF mice possess numerous SNPs that are distinct compared with C57/Bl6 mice (Doran et al., 2016). Within the last exon of *Ptgs2*, MOLF mice have 5 distinct SNPs that can be used to distinguish the C57/Bl6 and MOLF alleles. As outlined in Figure 4A, we crossed WT C57/Bl6 or *lincRNA-Cox2* KO C57/Bl6 mice with MOLF-WT mice to determine how loss of *lincRNA-Cox2* affects *Ptgs2*. By qRT-PCR, we show that *lincRNA-Cox2* expression is lost in the KO mice, whereas the native promoter is intact, represented by LacZ expression (Figures 4B and 4C). When examining the heterozygous mice, the MOLF-KO mice had reduced expression of *lincRNA-Cox2* and *Ptgs2* compared with MOLF-WT mice (Figures 4B and 4D). Using RNA-seq, we determined that only the *lincRNA-Cox2* KO allele (C57/Bl6) had decreased expression of *Ptgs2*. The MOLF-WT allele, which has an intact lincRNA-Cox2 gene, was unaffected by the loss of *lincRNA-Cox2* (Figures 4E and 4F). These results support the finding that *lincRNA-Cox2* functions to regulate the expression of *Ptgs2* on the same chromosome and is graphically summarized in Figure 4G.

Ptgs2 Expression Is Not Required for Transcriptional Activity of *lincRNA-Cox2*

Because *lincRNA-Cox2* and *Ptgs2* show parallel expression kinetics following an inflammatory stimulus (Carpenter et al., 2013), we wanted to explore whether the regulatory interaction between *lincRNA-Cox2* and *Ptgs2* was unidirectional or whether *Ptgs2* itself affects the expression levels of the lincRNA. In addition, we wanted to understand whether the effect on *Ptgs2* was responsible for the changes in inflammatory genes, such as *Il6*. To address this question, we crossed conditional *Ptgs2* flox/flox mice (Wang et al., 2009) to Vavi-Cre mice to delete *Ptgs2* in all hematopoietic cells. We generated BMDMs from these $Ptgs2^{f/f}$-Vavi-Cre mice and confirmed deficiency of *Ptgs2* by

(F and G) Cas9 KO cells were reconstituted using a lentiviral vector expressing full-length *lincRNA-Cox2*. *LincRNA-Cox2* (F) and *Ptgs2* (G) levels were measured by qRT-PCR.

(H) A schematic outlining the strategy to knock down *lincRNA-Cox2* expression using CRISPRi.

(I) University of California, Santa Cruz (UCSC) browser tracks indicating histone marks, H3K4me1 (enhancer), H3K4me3 (active transcript), and p300 peaks measured using ChIP in BMDMs and lungs are outlined.

(J) Schematic outlining the strategy to remove exon 2 of *lincRNA-Cox2* using CRISPR/Cas9.

(K and L) Control (Ctl) and exon 2 KO BMDMs were stimulated with LPS for 6 hr, and expression levels of *lincRNA-Cox2* (K) and *Ptgs2* (L) were measured by qRT-PCR.

(M and N) *lincRNA-Cox2* (M) and *Ptgs2* (N) levels were measured in 6-hr LPS-stimulated BMDMs following knockdown of *lincRNA-Cox2* using CRISPRi. Data represent 3 combined biological replicates representative of 3 individual experiments.

Error bars represent standard deviation of biological triplicates. Student's t tests were performed using GraphPad Prism. Asterisks indicate statistically significant differences between mouse lines (*$p \geq 0.05$, **$p \geq 0.01$, ***$p \geq 0.005$).

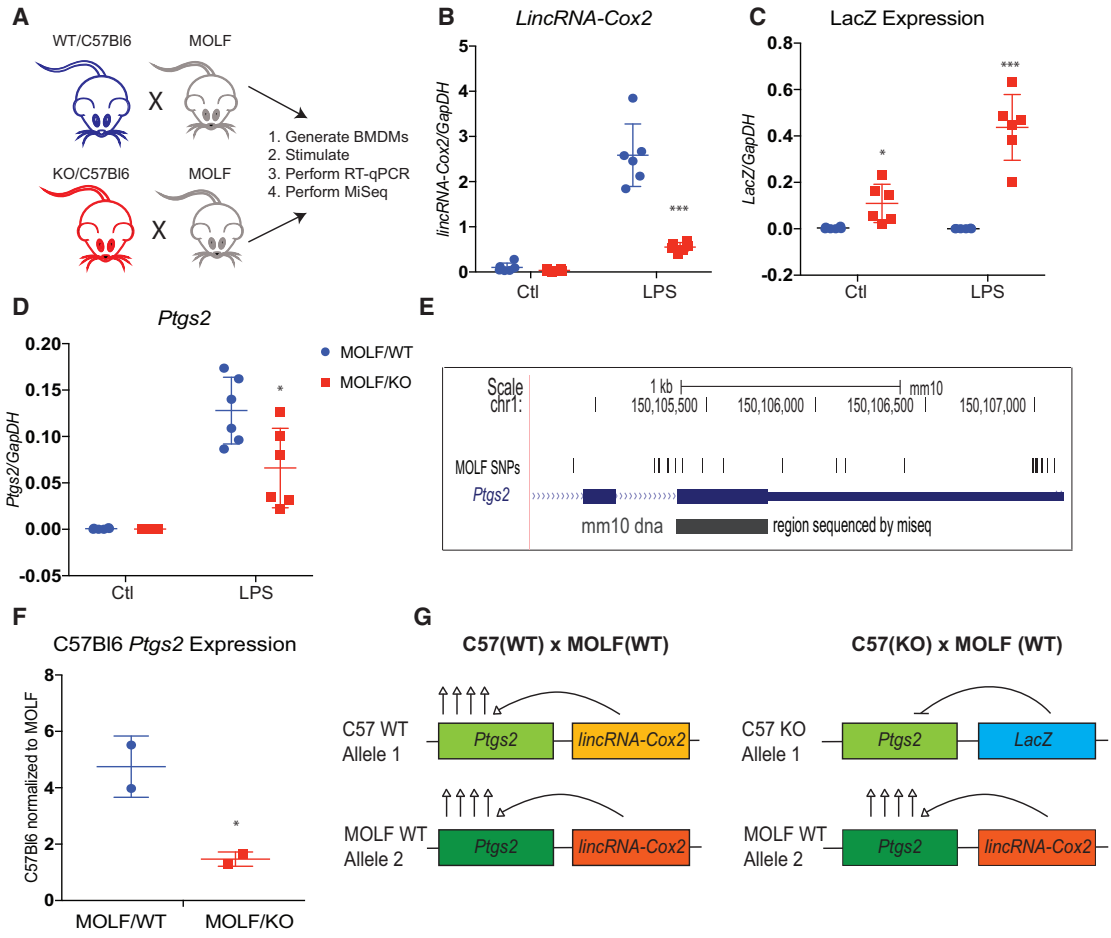

Figure 4. *lincRNA-Cox2* Influences the Expression of *Ptgs2* in *cis*

(A) Schematic outlining the mouse breeding and experimental strategy.

(B–D) Unstimulated and 6-hr LPS-stimulated BMDMs generated from heterozygous MOLF-WT and MOLF-KO mice and expression of *lincRNA-Cox2* (B), *Ptgs2* (C), and LacZ (D) were measured by qRT-PCR. Data represent 3 combined biological replicates representative of 3 individual experiments.

(E) UCSC genome browser tracks of MOLF SNPs compared with the C57/Bl6 mm10 genome build. The 414-bp region, highlighted in gray, is the targeted region of *Ptgs2* exon 10. The MOLF background has 5 distinct SNPs compared with the C57/Bl6 background.

(F) Sequenced reads of exon 10 from MOLF-WT and MOLF-KO mice were analyzed by normalizing the reads from the C57/Bl6 background to the MOLF background.

(G) Diagram explaining the results of why Ptgs2 is fully expressed in MOLF-WT mice and how Ptgs2 has repressed expression in MOLF-KO mice. LincRNA-Cox2 positively *cis*-regulates Ptgs2, whereas LacZ inhibits the expression of Ptgs2.

Error bars represent standard deviation of biological triplicates. Student's t tests were performed using GraphPad Prism7. Asterisks indicate statistically significant differences between mouse lines (*$p \geq 0.05$, ***$p \geq 0.005$).

immunoblotting and qRT-PCR in BMDMs stimulated with LPS (Figures 5A and 5B). The induction of *lincRNA-Cox2* proceeded normally in *Ptgs2*-deficient BMDMs (Figure 5C). Importantly, the induction of *Il6* and *Ifi202b*, which were both affected by *lincRNA-Cox2* deficiency, was normal in *Ptgs2*-deficient cells (Figures 5D and 5E). Together, these results suggest that the *lincRNA-Cox2* transcript can regulate genes in *trans* that are not normally regulated by *Ptgs2*. Thus, *lincRNA-Cox2* may represent an important modulator within and outside of the *Ptgs2* pathway.

Additionally, we used the BMDM CRISPRi clonal cell lines to target *Ptgs2* using two independent guide RNAs, as represented in Figure 5F. CRISPRi-mediated knockdown of *Ptgs2* by more than 90% had no effect on the transcription of *lincRNA-Cox2* upon LPS stimulation. These data further confirm that *Ptgs2*, RNA or protein, is not necessary for transcriptional activity of *lincRNA-Cox2* basally or after inflammatory stimulation (Figures 5G and 5H; Figures S6C and S6D), whereas *lincRNA-Cox2* is required for *Ptgs2* expression.

A *lincRNA-Cox2* Splicing Mutant Mouse Fails to Produce Any Inducible *lincRNA-Cox2* Transcript

To determine the *trans* functions of this lincRNA transcript independent of its role in regulating *Ptgs2*, we generated a mouse model with a deletion of the ~2.3-kb intronic region utilizing CRISPR/Cas9 (hereafter referred to as mutant mice). We

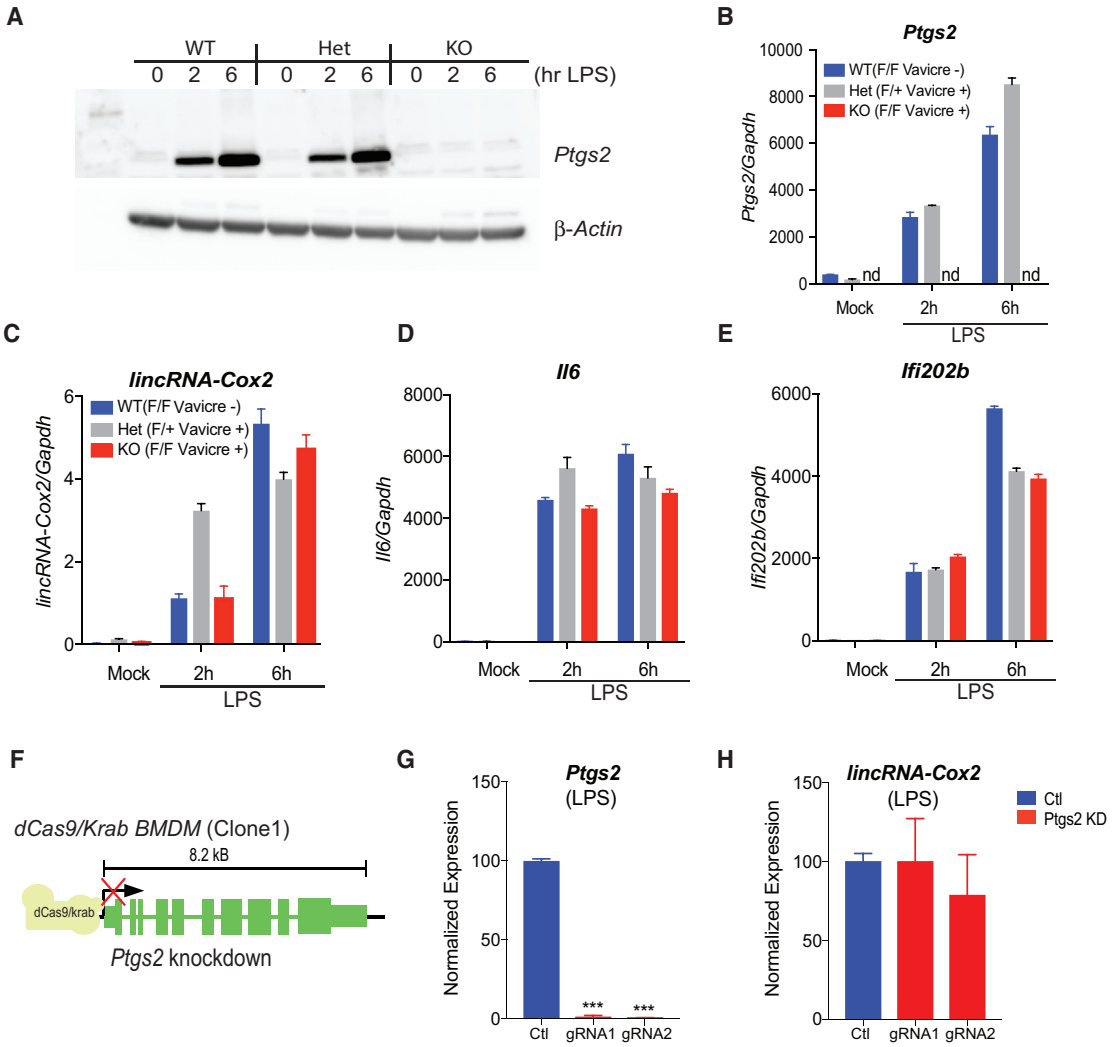

Figure 5. *Ptgs2* Does Not Affect the Expression of lincRNA-Cox2 or Its Target Genes

(A) BMDMs from WT, heterozygous (Het), and KO *Ptgs2* cells were stimulated with LPS. The levels of *Ptgs2* and *β-actin* were measured by western blot.

(B–E) BMDMs from WT, Het, and *Ptgs2* KO mice were stimulated with LPS for the indicated times, and the levels of *Ptgs2* (B), *lincRNA-Cox2* (C), *Il6* (D), and *Ifi202b* (E) were measured by qRT-PCR and normalized to *Gapdh*.

(F) Schematic of where dCas9-Krab will sit at the transcriptional start site of Ptgs2.

(G and H) qRT-PCR was used to measure *Ptgs2* (G), and *lincRNA-Cox2* (H) levels were measured in 6-hr LPS-stimulated BMDMs following knockdown of *lincRNA-Cox2* using CRISPRi clonal cell line 1. Data represent 3 combined biological replicates representative of 3 individual experiments.

Error bars represent standard deviation of biological triplicates. Student's t tests were performed using GraphPad Prism. Asterisks indicate statistically significant differences between mouse lines (***$p \geq 0.005$).

designed two guide RNAs targeting the 5′ and 3′ splice sites of *lincRNA-Cox2*. Exon 2 remained completely intact, whereas 50 bp were deleted from exon 1 (Figure 6A). PCR genotyping confirmed the mutant as described in Figure 6B. These mice were also born at expected Mendelian frequencies with no obvious developmental abnormities. We generated BMDMs from the mutant mice and examined the expression of *lincRNA-Cox2* in response to LPS challenge. Although the *lincRNA-Cox2* transcript was inducible following LPS stimulation in WT BMDM cells, there was only very low basal expression of *lincRNA-Cox2* in the mutant BMDM cells, as measured by qRT-PCR (Figure 6C).

In contrast to data we obtained with the full gene KO, *Ptgs2* levels were comparable between the WT and mutant BMDMs (Figure 6D). We next examined *Ptgs2* levels in tissues, specifically the lung, where *lincRNA-Cox2* is most highly expressed, and the spleen, where the majority of white blood cells are stored (Figures 2A, 2C, and 2E, Figure S1A). In the mutant, intron-less mouse, *lincRNA-Cox2* levels were dramatically reduced in the lung and spleen following LPS stimulation (Figures 6E and 6G). Again, there was no effect on *Ptgs2* levels within the lung and spleen of mutant mice (Figures 6F and 6H). These observations support the hypothesis that this locus can function as an enhancer to regulate *Ptgs2* and that this

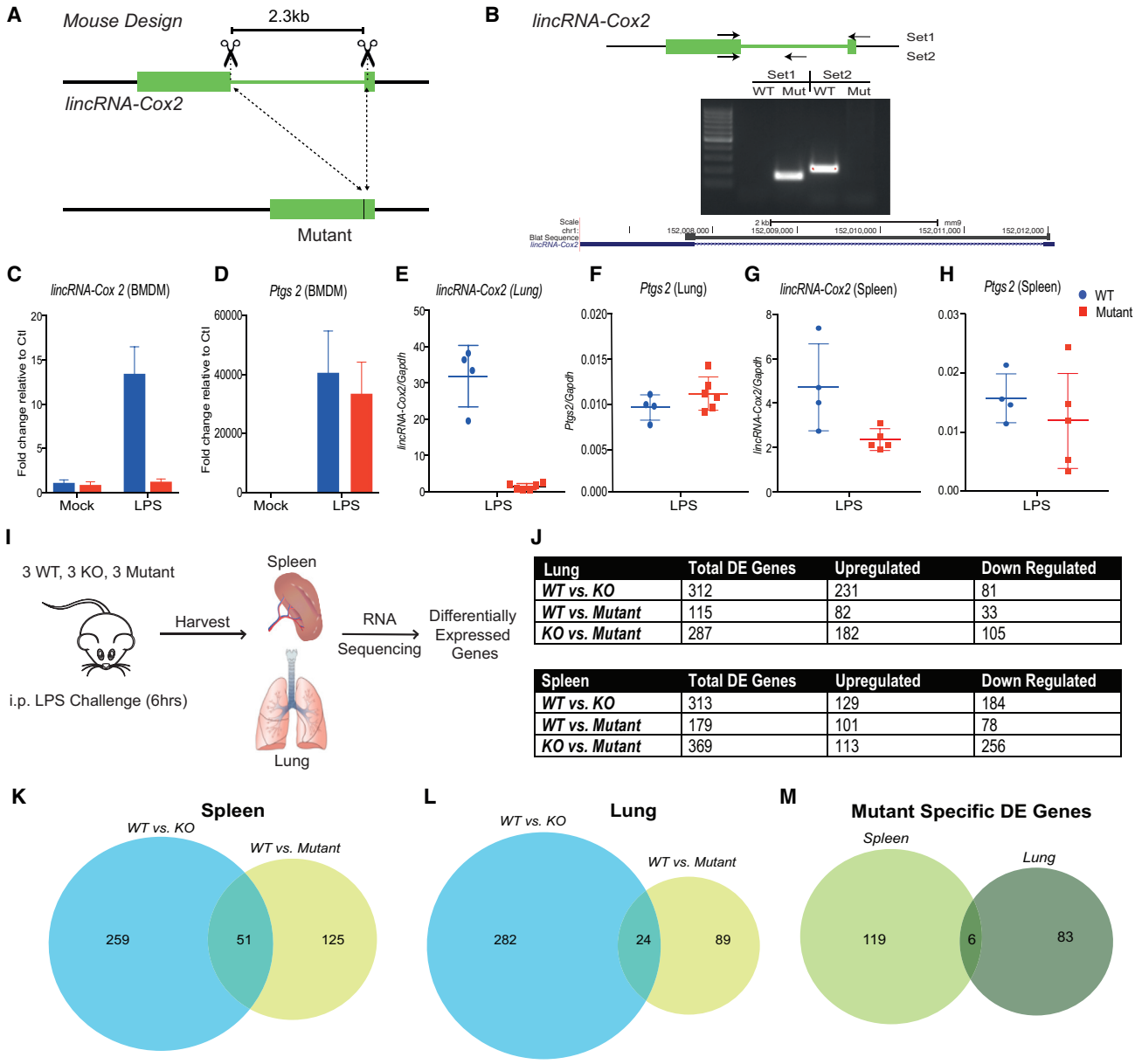

Lung	Total DE Genes	Upregulated	Down Regulated
WT vs. KO	312	231	81
WT vs. Mutant	115	82	33
KO vs. Mutant	287	182	105

Spleen	Total DE Genes	Upregulated	Down Regulated
WT vs. KO	313	129	184
WT vs. Mutant	179	101	78
KO vs. Mutant	369	113	256

Figure 6. A Lung-Specific Role for *lincRNA-Cox2* Acting in *trans*

(A) Schematic outlining the strategy to remove the intron of *lincRNA-Cox2* using CRISPR/Cas9 to generate mutant mice.

(B) Genotyping data confirming the mutation within the *lincRNA-Cox2* locus.

(C and D) BMDMs were isolated from WT and mutant mice and stimulated with LPS or Mock (water), and *lincRNA-Cox2* (C) and *Ptgs2* (D) levels were measured by qRT-PCR. Error bars represent standard deviation of biological triplicates.

(E–H) WT and mutant mice were challenged with 20 mg/kg LPS for 6 hr, and lungs and spleens were removed. *lincRNA-Cox2* (E and G) and *Ptgs2* (F and H) levels were measured by qRT-PCR.

(I) Experimental schematic outlining the sequencing strategy of *in vivo* experiment comparing WT, KO, and mutant mice.

(J) Tables highlighting the number of genes differentially expressed determined using DESeq (cutoff of 1.5 log2 fold change in expression with $p > 0.05$) (DE in either the lung or spleen when comparing WT, KO, and mutant expression profiles after LPS treatment).

(K–M) Venn diagrams displaying the DE genes from spleen (K) or lung (L) that overlap between mutant and KO or overlap between mutant DE genes from the spleen and lung (M).

eRNA activity is maintained in this model. The enhancer located prior to the start site of the locus in conjunction with the basal transcript work together to mediate these effects on *Ptgs2*.

lincRNA-Cox2 Regulates Distinct Sets of Genes in the Lung and Spleen

Now having two separate mouse models, a complete deletion KO mouse, and an intron-less mutant mouse, we asked whether

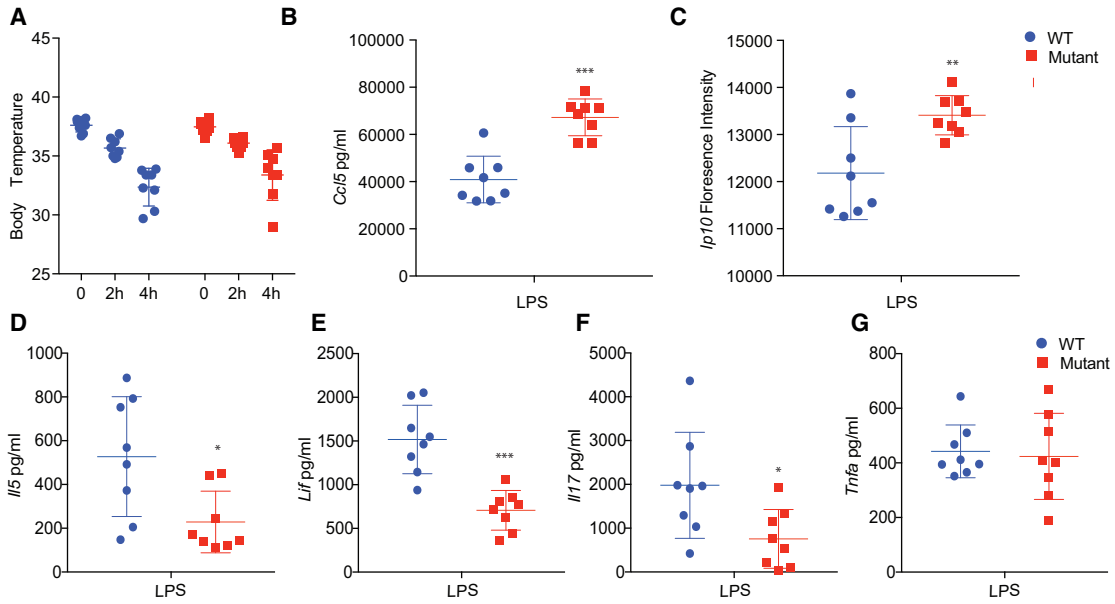

Figure 7. *lincRNA-Cox2* Controls Innate Immune Cells in *trans In Vivo*

(A–G) WT and Mutant mice were challenged with 20 mg/kg LPS, and body temperature was measured (A). Mice were sacrificed after 6 hr, cardiac punctures were performed, serum was isolated, and multiplex cytokine analysis was performed for *Ccl5* (B), *Ip10* (C), *Il5* (D), *Lif* (E), *Il17* (F), and *Tnfa* (G). Each dot represents an individual animal. Error bars represent standard deviation of biological triplicates. Student's t tests were performed using GraphPad Prism. Asterisks indicate statistically significant differences between mouse lines (*p ≥ 0.05, **p ≥ 0.01, ***p ≥ 0.005).

the absence of the *lincRNA-Cox2* transcript has a *trans* and organ-specific role *in vivo*. lincRNA-Cox2 is expressed at high levels in the lung and very low in the spleen (Figures 2D and 2E; Figure S1A). The expression of *lincRNA-Cox2* is inducible upon LPS challenge in the spleen and slightly reduced in the lung (Figures 2D and 2E). To define the global regulatory role of *lincRNA-Cox2*, we challenged WT, KO, and mutant mice by i.p. injection of *E. coli* LPS for 6 hr, followed by RNA-seq of the spleen and lung, as represented in Figure 6I.

DESeq2 analysis was used to determine the differentially expressed (DE) genes between WT versus KO, WT versus mutant, or KO versus mutant in both the lung and spleen (Figure 6J). The KO versus WT mice had 312 DE genes in the lung and 313 DE genes in the spleen (Figure 6J). The mutant versus WT mice had 115 DE genes in the lung and 179 DE genes in the spleen (Figure 6J). When comparing gene expression of mutant mice with KO mice, there were hundreds of significantly DE genes, reinforcing that these mice had very distinct phenotypes from one another because of the *cis* and *trans* functions of *lincRNA-Cox2* (Figures 6J–6L). Interestingly, when comparing mutant *lincRNA-Cox2*-specific DE genes, there are only six that overlap between the spleen and lung (Figure 6M). Of these six genes, only one gene changed from being upregulated to downregulated from the spleen to the lung, *Ptprh* (synonym Sap-1) (Figure S7C; Bujko et al., 2017). Database for Annotation, Visualization, and Integrated Discovery (DAVID) analysis of the differentially expressed genes of the spleen and lung show similar pathways, such as glycoprotein and inflammatory response, as well distinct pathways, such as fibronectin and heparin binding in the spleen or cellular homeostasis and secretory granule pathways in the lung (Figures S7A and S7B). *LincRNA-Cox2* is highly expressed in the lung in a very cell type-specific manner (Figures S1B and S1C). Using the Mouse Cell Atlas generated by Han et al., 2018, we can show the differences in cell type expression between *Ptgs2* and *lincRNA-Cox2* (Figure S1B). Overall, *lincRNA-Cox2* has a higher expression in specific immune-related cells in the lung, whereas *Ptgs2* has higher expression in epithelial and endothelial cells, providing additional evidence that *lincRNA-Cox2* has distinct roles in *trans* independent of its regulation of *Ptgs2*.

lincRNA-Cox2 Controls Immune Genes in *trans* Independent of *Ptgs2* following LPS Challenge *In Vivo*

The generation of the mutant intron-less *lincRNA-Cox2* loss-of-function model allowed us to assess the contribution of the lincRNA transcript *in vivo* independent of the *cis* effect on *Ptgs2*. We asked whether the absence of the *lincRNA-Cox2* transcript affects *in vivo* responses to LPS. We challenged the *lincRNA-Cox2* mutant mice *in vivo* by i.p. injection of *E. coli* LPS. The temperature of the mice, a clinical parameter of septic shock, decreased over time in both strains (Figure 7A). Serum cytokines were then measured using multiplex assays. Interferon-stimulated genes, including *Ccl5* (Rantes) and *Ip10*, were both found at elevated levels in the *lincRNA-Cox2* mutant mice following LPS challenge (Figures 7B and 7C), whereas proinflammatory gene expression, including *Il5*, *Lif*, and *Il17*, was reduced (Figures 7D–7F). *Tnfα* expression levels were unchanged in control and mutant mice (Figure 7G). These *in vivo* data are consistent with published *in vitro* data showing that *lincRNA-Cox2* can act to both promote and inhibit the expression of innate immune

genes. Because all genes affected in the mutant mice were located on different chromosomes to *lincRNA-Cox2* (chromosome 1), these data confirm that *lincRNA-Cox2* functions in *trans* to control immune responses *in vivo*.

DISCUSSION

lincRNAs remain an understudied class of genes specifically in the context of the immune system. Although there are a number of studies, both by our lab and others, showing that *lincRNA-Cox2* promotes and restrains different classes of innate immune gene expression, none have shown the function of this gene *in vivo* (Carpenter et al., 2013; Covarrubias et al., 2017; Hu et al., 2016; Tong et al., 2016; Xue et al., 2018). Here we expand our knowledge of the role of *lincRNA-Cox2* by generating two murine models and multiple macrophage cell lines, which strengthens our earlier findings that *lincRNA-Cox2* can inhibit expression of ISGs and enhance pro-inflammatory gene expression. In addition, we now reveal that *lincRNA-Cox2* also functions through an eRNA mechanism to control the expression of the neighboring gene *Ptgs2* (Cox2) *in vivo*.

We initially characterized the *lincRNA-Cox2* KO mouse, generated by replacing the locus with LacZ, by tracking LacZ expression in organs after LPS challenge. We observed that *lincRNA-Cox2* was highly expressed in the lung, and further analysis of RNA-seq data confirmed this observation. To determine how loss of *lincRNA-Cox2* expression affects gene expression at steady state, we performed RNA-seq on lung samples comparing WT and KO. We were intrigued to identify *Ptgs2* among the most significantly altered transcripts in the KO lung. Our previous work using shRNA-mediated knockdown of *lincRNA-Cox2* had not revealed any change in the expression levels of *Ptgs2* in BMDMs (Carpenter et al., 2013), suggesting that this *cis* activity was carried out through an enhancer within the DNA of this locus. We were unable to rescue the expression of *Ptgs2* by ectopic overexpression of *lincRNA-Cox2*, further suggesting that it is either the DNA responsible for the phenotype or that locus-specific expression of the transcript is required for this function. A caveat with the reconstitution experiment is that we express *lincRNA-Cox2* off a plasmid using an EF1α promoter. Although the reconstituted *lincRNA-Cox2* localizes to the nucleus and cytoplasm in a similar manner as the native transcript, it is no longer induced by its native promoter or undergoing splicing. Additional experiments, including ectopic expression of *lincRNA-Cox2* with the native promoter or the entire locus, could help determine whether these features are critical for the function of *lincRNA-Cox2* in controlling *Ptgs2* in *cis*. The majority of the sequence for *lincRNA-Cox2* lies within exon 2, and removing this exon using CRISPR resulted in a dramatic decrease in *Ptgs2*. However, when we examined the locus for enhancer elements, we did not identify any within exon 2 of the gene. Instead, we observed evidence for DNA enhancer elements that lie only within the promoter of *lincRNA-Cox2*, including H3K4 mono-methylation (H3K4me1) and p300 ChIP-seq. Interestingly, this enhancer region remained intact in the *lincRNA-Cox2* KO mouse, and the locus was transcriptionally active, but *Ptgs2* was downregulated. This indicates that locus-specific transcription of *lincRNA-Cox2* is required to mediate the activity in *cis*, suggesting that *lincRNA-Cox2* functions as a form of eRNA.

It has been reported that many lincRNAs act locally, explaining why lincRNAs, like *lincRNA-Cox2*, display a similar expression pattern as their neighboring protein-coding genes. A recent study by Engreitz et al. (2016) showed that lncRNA and protein-coding genes can function locally and affect each other's expression levels. They show that 5 of 12 lincRNA loci they studied affected their neighboring gene in *cis* either through enhancer activity from within the promoter through the act of transcription or the act of splicing of the lincRNA (Engreitz et al., 2016).

eRNAs are produced from transcriptionally active enhancer regions, which are epigenetically defined by high levels of H3K4me1, low levels of H3K4 trimethyl (H3K4me3), and high levels of histone 3 lysine 27 acetylation (H3K27Ac) (Creyghton et al., 2010; Heintzman et al., 2007; Visel et al., 2009). lincRNAs that function in *cis* to either enhance or suppress the expression of neighboring protein-coding genes can be classified as enhancer or repressor RNAs. Studies from Ilott et al., 2014 identified over 40 canonical lincRNAs that act as eRNAs to regulate protein-coding genes upon LPS stimulation in human monocytes. Interestingly, although we found that knocking out *lincRNA-Cox2* greatly affected *Ptgs2*, deletion of *Ptgs2* itself did not affect basal or inducible levels of *lincRNA-Cox2*, showing that the effects are not reciprocal between these two loci. This result was further confirmed using CRISPRi, which mediates heterochromatin formation and silencing of gene transcription. Knocking down the transcription of *Ptgs2* by over 90% had no effect on the regulation of *lincRNA-Cox2*. The *lincRNA-Cox2* locus has both high H3K4me1 and H3K4me3 marks, making it distinct from the typical definition of eRNAs. It is possible that, as the field and function of lncRNAs continues to grow, that the categories that define their functions will also expand.

To determine whether transcription of *lincRNA-Cox2* is important to regulate *Ptgs2*, we knocked down expression of the gene using CRISPRi. Our data show that we can knock down *lincRNA-Cox2* expression more than 95%, which equally affects *Ptgs2* expression by more than 95%. In addition, using active Cas9, we knocked out exon 2 of *lincRNA-Cox2* (the majority of the *lincRNA-Cox2* sequence), this perturbation also affected *Ptgs2* expression. Because we did not identify any possible enhancer marks within exon 2, and all of the enhancer marks were within the promoter, we conclude that *lincRNA-Cox2* is functioning through an eRNA mechanism to control *Ptgs2*. Although unlikely, it is possible that there is an unidentified enhancer mark within the DNA of exon 2. Future work aimed at inserting stop cassettes within exon 2 could confirm that, indeed, transcription of the gene is essential for *Ptgs2* levels. The data we generated from our "intron-less splicing mutant" mice strongly suggest that this is the case. We used CRISPR/Cas9 to generate the mutant mouse. In this mouse, the exons of the *lincRNA-Cox2* transcript are maintained; however, the intron and splice sites are removed. This mouse expressed basal levels of *lincRNA-Cox2*; however, the transcript is no longer inducible following LPS stimulation. It is possible that, because this transcript is no longer undergoing

splicing, that it is highly unstable and, therefore, rapidly degraded following LPS stimulation. In the future, northern blots should be performed to confirm there are no additional unexpected lincRNA fragments in this model. Effectively, this mouse functions as a transcript loss-of-function mouse model of *lincRNA-Cox2*. Our studies with BMDMs and mice *in vivo* suggest that splicing is not required for the observed effect on *Ptgs2*. Low basal expression of the spliced *lincRNA-Cox2* transcript is sufficient to activate the *Ptgs2* locus, further suggesting that, indeed, this gene can function through an eRNA mechanism.

A final experiment was performed to assess whether *lincRNA-Cox2* is regulating *Ptgs2* on the same chromosome. We crossed our C57/Bl6 WT and KO mice with MOLF mice, which contain millions of SNPs, allowing us to differentiate between the two alleles. Studying the *Ptgs2* locus, we found that only expression from the *cis* (C57/Bl6) allele was affected when *lincRNA-Cox2* was knocked out. These data confirmed that indeed *lincRNA-Cox2* functions to regulate *Ptgs2* on the same chromosome. We predict that *lincRNA-Cox2* is functioning as an eRNA and the RNA is tethering the enhancer to the *Ptgs2* locus and forming a topologically associating domain. Further work including performing 3C/Hi-C should confirm this.

The lincRNA-Cox2 mutant mice are a critical model enabling us to study the *trans* activity for *lincRNA-Cox2* independent of its effects on *Ptgs2*. As mentioned previously, this mouse functions as a transcript loss-of-function mouse model of *lincRNA-Cox2*. The original *lincRNA-Cox2* KO mouse not only attenuated the expression of *lincRNA-Cox2* but also repressed the expression of *Ptgs2*, whereas this model only affects *lincRNA-Cox2* levels, enabling us to use these models to distinguish between the *cis* and *trans* functions for this gene.

Distinct tissue-specific functions have been shown for several lincRNAs. One such example is NEAT1, which is critical for synapse formation in the brain (Sunwoo et al., 2017), whereas, in adipose tissue, NEAT1 is necessary for the differentiation of white adipocytes (Cooper et al., 2014). *lincRNA-Cox2* KO and mutant mice were used to globally study the *cis* and *trans* role of *lincRNA-Cox2 in vivo* by performing RNA-seq on lungs and spleens from LPS-challenged WT, KO, and mutant mice. Not surprisingly, we observed over 300 genes that were differentially regulated when comparing KO with WT mice, whereas only half that number were affected when comparing mutants with the WT. We believe that this is due to the fact that the mutant mice reveal only the functions of lincRNA-Cox2 in *trans*, whereas the KO mice exhibit both *cis* effects on *Ptgs2* and *trans* effects.

Interestingly, the mutant mice possessed differentially expressed genes in the lung and spleen, emphasizing a possible organ-specific role for *lincRNA-Cox2*. Indeed, we observe very high levels of *lincRNA-Cox2* in the lung, whereas the transcript is only induced in the spleen following inflammatory stimulation. Further work will be needed to understand mechanistically how *lincRNA-Cox2* affects inflammatory responses in the lung and spleen. From our LacZ staining within the lung, combined with data from the mouse cell atlas, we observe cell type-specific expression patterns for *lincRNA-Cox2*. In the future, it will be informative to isolate these specific cells for further mechanistic studies.

Finally, we wanted to determine whether *lincRNA-Cox2* can affect gene expression in the periphery following LPS challenge *in vivo*. We observe an increase in *Ccl5* and *Ip10* (*Cxcl10*) levels and a decrease in *Il5*, *Il17*, and *Lif* levels in the serum of mice following endotoxic shock, suggesting that *lincRNA-Cox2* can function in *trans* to control various innate immune genes. These data highlight two important features of this lincRNA's function: the *in vivo* immune-regulatory activity of *lincRNA-Cox2* on immune gene expression and the role of the *lincRNA-Cox2* locus in controlling *Ptgs2* (Cox2) levels. Together, these studies further our understanding of how lincRNAs can function both in *cis* and in *trans* to control gene expression, findings that are only evident through the use of multiple complimentary genetic perturbations. The drastic influence of non-coding genes on key immune signaling axes, such as the prostaglandin pathway as shown here, has broad translational implications because it indicates that protein-centered sequencing approaches are likely insufficient to fully understand genetically mediated autoimmune and auto-inflammatory conditions. Large-scale functional validations of noncoding mutations, facilitated by CRISPR/Cas9, will provide a promising approach to better understand the pathogenesis of inflammatory and non-inflammatory diseases. CRISPR/Cas9 technology has revolutionized the field of genome editing and will be a critical tool moving forward to enable rapid generation of animal models to fully characterize any lincRNA locus.

STAR★METHODS

Detailed methods are provided in the online version of this paper and include the following:

- KEY RESOURCES TABLE
- CONTACT FOR RESOURCE AND SHARING
- EXPERIMENTAL MODEL AND SUBJECT DETAILS
  - Maintenance of mice
  - LincRNA-Cox2 KO mice
  - Ptgs2 (Cox2) f/f VavCre mice
  - CRISPR/Cas9-mediated generation of LincRNA-Cox2 intron-less mice
  - Cell culture and BMDM differentiation
- METHOD DETAILS
  - LPS shock model
  - *In vitro* stimulation of BMDMs
  - Transfection and stable lentiviral overexpression of lincRNA-Cox2
  - CRISPR/Cas9 mediated deletion of lincRNA-Cox2 in immortalized BMDMs
  - CRISPRi mediated KO of lincRNA-Cox2 and Ptgs2 in immortalized BMDMs
  - RNA isolation and cDNA synthesis and RT-qPCR
  - RNA-Sequencing
  - MiSeq
  - Measurement of prostaglandins by mass spectrometry
  - Western Blot Analysis
  - LacZ staining
- QUANTIFICATION AND STATISTICAL ANALYSIS
  - For *in vivo* studies
  - For *in vitro* studies
- DATA AVAILABILITY

SUPPLEMENTAL INFORMATION

Supplemental Information includes seven figures and seven tables and can be found with this article online at https://doi.org/10.1016/j.celrep.2018.10.027.

ACKNOWLEDGMENTS

This work is supported by grants from the NIH (R56 AI127414 to S. Carpenter; AI115448, AI079293, and R37 AI067497 to K.A.F.; R01 GM110251 to M.T.M., and T32 GM008646 to E.K.R.); a postdoctoral fellowship from the German Research Foundation (DFG EL 790/1-1); and the Berta Ottenstein Programme, Faculty of Medicine, University of Freiburg to R.E.

AUTHOR CONTRIBUTIONS

S. Carpenter and K.A.F. conceived and coordinated the project. S. Carpenter, K.A.F., and E.K.R. wrote the manuscript. R.E., S. Carpenter, and E.K.R. oversaw the majority of the work. R.E. performed qRT-PCR and western blotting. E.K.R. generated the CRISPRi data, performed qRT-PCRs, and carried out *in vivo* studies. B.S. and S. Carpenter performed qRT-PCRs and carried out *in vivo* studies. S.C.L. performed RNA-seq and LacZ staining. A.F.G. and S.K. performed analyses of RNA-seq data. Z.J. performed studies on Ptgs2 KO animals. J.L.R. generated *lincRNA-Cox2* KO mice and provided intellectual input. S. Covarrubias assisted with the generation of KOs using CRISPR/Cas9. E.J.H. and G.A.F. performed mass spectrometry analyses. S.A., M.M., J.C., and S.S. provided technical assistance for Figure 2. M.T.M. provided critical reagents and suggestions. All authors reviewed the results and approved the final version of the manuscript.

DECLARATION OF INTERESTS

The authors declare no competing interests.

Received: October 19, 2017
Revised: September 4, 2018
Accepted: October 3, 2018
Published: November 6, 2018

REFERENCES

Anderson, D.M., Anderson, K.M., Chang, C.-L., Makarewich, C.A., Nelson, B.R., McAnally, J.R., Kasaragod, P., Shelton, J.M., Liou, J., Bassel-Duby, R., and Olson, E.N. (2015). A micropeptide encoded by a putative long noncoding RNA regulates muscle performance. Cell *160*, 595–606.

Anderson, K.M., Anderson, D.M., McAnally, J.R., Shelton, J.M., Bassel-Duby, R., and Olson, E.N. (2016). Transcription of the non-coding RNA upperhand controls Hand2 expression and heart development. Nature *539*, 433–436.

Atianand, M.K., Hu, W., Satpathy, A.T., Shen, Y., Ricci, E.P., Alvarez-Dominguez, J.R., Bhatta, A., Schattgen, S.A., McGowan, J.D., Blin, J., et al. (2016). A Long Noncoding RNA lincRNA-EPS Acts as a Transcriptional Brake to Restrain Inflammation. Cell *165*, 1672–1685.

Bassett, A.R., Akhtar, A., Barlow, D.P., Bird, A.P., Brockdorff, N., Duboule, D., Ephrussi, A., Ferguson-Smith, A.C., Gingeras, T.R., Haerty, W., et al. (2014). Considerations when investigating lncRNA function in vivo. eLife *3*, e03058.

Blasi, E., Radzioch, D., Merletti, L., and Varesio, L. (1989). Generation of macrophage cell line from fresh bone marrow cells with a myc/raf recombinant retrovirus. Cancer Biochem. Biophys *10*, 303–317.

Bujko, M., Kober, P., Statkiewicz, M., Mikula, M., Grecka, E., Rusetska, N., Ligaj, M., Ostrowski, J., and Siedlecki, J.A. (2017). Downregulation of PTPRH (Sap-1) in colorectal tumors. Int. J. Oncol. *51*, 841–850.

Carmona, S., Lin, B., Chou, T., Arroyo, K., and Sun, S. (2018). LncRNA Jpx induces Xist expression in mice using both trans and cis mechanisms. PLoS Genet. *14*, e1007378.

Carpenter, S., Aiello, D., Atianand, M.K., Ricci, E.P., Gandhi, P., Hall, L.L., Byron, M., Monks, B., Henry-Bezy, M., Lawrence, J.B., et al. (2013). A long noncoding RNA mediates both activation and repression of immune response genes. Science *341*, 789–792.

Cooper, D.R., Carter, G., Li, P., Patel, R., Watson, J.E., and Patel, N.A. (2014). Long Non-Coding RNA NEAT1 Associates with SRp40 to Temporally Regulate PPARγ2 Splicing during Adipogenesis in 3T3-L1 Cells. Genes (Basel) *5*, 1050–1063.

Covarrubias, S., Robinson, E.K., Shapleigh, B., Vollmers, A., Katzman, S., Hanley, N., Fong, N., McManus, M.T., and Carpenter, S. (2017). CRISPR/Cas-based screening of long non-coding RNAs (lncRNAs) in macrophages with an NF-κB reporter. J. Biol. Chem. *292*, 20911–20920.

Creyghton, M.P., Cheng, A.W., Welstead, G.G., Kooistra, T., Carey, B.W., Steine, E.J., Hanna, J., Lodato, M.A., Frampton, G.M., Sharp, P.A., et al. (2010). Histone H3K27ac separates active from poised enhancers and predicts developmental state. Proc. Natl. Acad. Sci. USA *107*, 21931–21936.

Doran, A.G., Wong, K., Flint, J., Adams, D.J., Hunter, K.W., and Keane, T.M. (2016). Deep genome sequencing and variation analysis of 13 inbred mouse strains defines candidate phenotypic alleles, private variation and homozygous truncating mutations. Genome Biol. *17*, 167.

ENCODE Project Consortium (2012). An integrated encyclopedia of DNA elements in the human genome. Nature *489*, 57–74.

Engreitz, J.M., Pandya-Jones, A., McDonel, P., Shishkin, A., Sirokman, K., Surka, C., Kadri, S., Xing, J., Goren, A., Lander, E.S., et al. (2013). The Xist lncRNA exploits three-dimensional genome architecture to spread across the X chromosome. Science *341*, 1237973.

Engreitz, J.M., Haines, J.E., Perez, E.M., Munson, G., Chen, J., Kane, M., McDonel, P.E., Guttman, M., and Lander, E.S. (2016). Local regulation of gene expression by lncRNA promoters, transcription and splicing. Nature *539*, 452–455.

Gajewski, T.F., Schreiber, H., and Fu, Y.-X. (2013). Innate and adaptive immune cells in the tumor microenvironment. Nat. Immunol. *14*, 1014–1022.

Gierut, A., Perlman, H., and Pope, R.M. (2010). Innate immunity and rheumatoid arthritis. Rheum. Dis. Clin. North Am. *36*, 271–296.

Gomez, J.A., Wapinski, O.L., Yang, Y.W., Bureau, J.F., Gopinath, S., Monack, D.M., Chang, H.Y., Brahic, M., and Kirkegaard, K. (2013). The NeST long ncRNA controls microbial susceptibility and epigenetic activation of the interferon-γ locus. Cell *152*, 743–754.

Groff, A.F., Sanchez-Gomez, D.B., Soruco, M.M.L., Gerhardinger, C., Barutcu, A.R., Li, E., Elcavage, L., Plana, O., Sanchez, L.V., Lee, J.C., et al. (2016). In Vivo Characterization of Linc-p21 Reveals Functional cis-Regulatory DNA Elements. Cell Rep. *16*, 1–9.

Grote, P., Wittler, L., Hendrix, D., Koch, F., Währisch, S., Beisaw, A., Macura, K., Bläss, G., Kellis, M., Werber, M., and Herrmann, B.G. (2013). The tissue-specific lncRNA Fendrr is an essential regulator of heart and body wall development in the mouse. Dev. Cell *24*, 206–214.

Guttman, M., Amit, I., Garber, M., French, C., Lin, M.F., Feldser, D., Huarte, M., Zuk, O., Carey, B.W., Cassady, J.P., et al. (2009). Chromatin signature reveals over a thousand highly conserved large non-coding RNAs in mammals. Nature *458*, 223–227.

Han, X., Wang, R., Zhou, Y., Fei, L., Sun, H., Lai, S., Saadatpour, A., Zhou, Z., Chen, H., Ye, F., et al. (2018). Mapping the Mouse Cell Atlas by Microwell-Seq. Cell *172*, 1091–1107.e17.

Heintzman, N.D., Stuart, R.K., Hon, G., Fu, Y., Ching, C.W., Hawkins, R.D., Barrera, L.O., Van Calcar, S., Qu, C., Ching, K.A., et al. (2007). Distinct and predictive chromatin signatures of transcriptional promoters and enhancers in the human genome. Nat. Genet. *39*, 311–318.

Hu, G., Gong, A.-Y., Wang, Y., Ma, S., Chen, X., Chen, J., Su, C.-J., Shibata, A., Strauss-Soukup, J.K., Drescher, K.M., and Chen, X.M. (2016). LincRNA-Cox2 Promotes Late Inflammatory Gene Transcription in Macrophages through Modulating SWI/SNF-Mediated Chromatin Remodeling. J. Immunol. *196*, 2799–2808.

Ilott, N.E., Heward, J.A., Roux, B., Tsitsiou, E., Fenwick, P.S., Lenzi, L., Goodhead, I., Hertz-Fowler, C., Heger, A., Hall, N., et al. (2014). Long non-coding

RNAs and enhancer RNAs regulate the lipopolysaccharide-induced inflammatory response in human monocytes. Nat. Commun. *5*, 3979.

Jégu, T., Aeby, E., and Lee, J.T. (2017). The X chromosome in space. Nat. Rev. Genet. *18*, 377–389.

Joung, J., Engreitz, J.M., Konermann, S., Abudayyeh, O.O., Verdine, V.K., Aguet, F., Gootenberg, J.S., Sanjana, N.E., Wright, J.B., Fulco, C.P., et al. (2017). Genome-scale activation screen identifies a lncRNA locus regulating a gene neighbourhood. Nature *548*, 343–346.

Kawasaki, N., Miwa, T., Hokari, S., Sakurai, T., Ohmori, K., Miyauchi, K., Miyazono, K., and Koinuma, D. (2018). Long noncoding RNA NORAD regulates transforming growth factor-β signaling and epithelial-to-mesenchymal transition-like phenotype. Cancer Sci. *109*, 2211–2220.

Kim, T.-K., Hemberg, M., and Gray, J.M. (2015). Enhancer RNAs: a class of long noncoding RNAs synthesized at enhancers. Cold Spring Harb. Perspect. Biol. *7*, a018622.

Kopp, F., and Mendell, J.T. (2018). Functional Classification and Experimental Dissection of Long Noncoding RNAs. Cell *172*, 393–407.

Kotzin, J.J., Spencer, S.P., McCright, S.J., Kumar, D.B.U., Collet, M.A., Mowel, W.K., Elliott, E.N., Uyar, A., Makiya, M.A., Dunagin, M.C., et al. (2016). The long non-coding RNA Morrbid regulates Bim and short-lived myeloid cell lifespan. Nature *537*, 239–243.

Kretz, M., Siprashvili, Z., Chu, C., Webster, D.E., Zehnder, A., Qu, K., Lee, C.S., Flockhart, R.J., Groff, A.F., Chow, J., et al. (2013). Control of somatic tissue differentiation by the long non-coding RNA TINCR. Nature *493*, 231–235.

Lara-Astiaso, D., Weiner, A., Lorenzo-Vivas, E., Zaretsky, I., Jaitin, D.A., David, E., Keren-Shaul, H., Mildner, A., Winter, D., Jung, S., et al. (2014). Immunogenetics. Chromatin state dynamics during blood formation. Science *345*, 943–949.

Lee, S., Kopp, F., Chang, T.-C., Sataluri, A., Chen, B., Sivakumar, S., Yu, H., Xie, Y., and Mendell, J.T. (2016). Noncoding RNA NORAD Regulates Genomic Stability by Sequestering PUMILIO Proteins. Cell *164*, 69–80.

Li, H., Handsaker, B., Wysoker, A., Fennell, T., Ruan, J., Homer, N., Marth, G., Abecasis, G., and Durbin, R. (2009). The Sequence Alignment/Map format and SAMtools. Bioinformatics *25*, 2078–2079.

Li, Q., Su, Z., Xu, X., Liu, G., Song, X., Wang, R., Sui, X., Liu, T., Chang, X., and Huang, D. (2012). AS1DHRS4, a head-to-head natural antisense transcript, silences the DHRS4 gene cluster in cis and trans. Proc. Natl. Acad. Sci. USA *109*, 14110–14115.

Liang, W.-C., Ren, J.-L., Wong, C.-W., Chan, S.-O., Waye, M.M.-Y., Fu, W.-M., and Zhang, J.-F. (2018). LncRNA-NEF antagonized epithelial to mesenchymal transition and cancer metastasis via cis-regulating FOXA2 and inactivating Wnt/β-catenin signaling. Oncogene *37*, 1445–1456.

Liu, S.J., Horlbeck, M.A., Cho, S.W., Birk, H.S., Malatesta, M., He, D., Attenello, F.J., Villalta, J.E., Cho, M.Y., Chen, Y., et al. (2017). CRISPRi-based genome-scale identification of functional long noncoding RNA loci in human cells. Science *355*, aah7111.

Love, M.I., Huber, W., and Anders, S. (2014). Moderated estimation of fold change and dispersion for RNA-seq data with DESeq2. Genome Biol. *15*, 550.

Masters, S.L., Simon, A., Aksentijevich, I., and Kastner, D.L. (2009). Horror autoinflammaticus: the molecular pathophysiology of autoinflammatory disease (*). Annu. Rev. Immunol. *27*, 621–668.

Melo, C.A., Drost, J., Wijchers, P.J., van de Werken, H., de Wit, E., Oude Vrielink, J.A.F., Elkon, R., Melo, S.A., Léveillé, N., Kalluri, R., et al. (2013). eRNAs are required for p53-dependent enhancer activity and gene transcription. Mol. Cell *49*, 524–535.

Morris, K.V., and Mattick, J.S. (2014). The rise of regulatory RNA. Nat. Rev. Genet. *15*, 423–437.

Neumann, P., Jaé, N., Knau, A., Glaser, S.F., Fouani, Y., Rossbach, O., Krüger, M., John, D., Bindereif, A., Grote, P., et al. (2018). The lncRNA GATA6-AS epigenetically regulates endothelial gene expression via interaction with LOXL2. Nat. Commun. *9*, 237.

Ørom, U.A., Derrien, T., Beringer, M., Gumireddy, K., Gardini, A., Bussotti, G., Lai, F., Zytnicki, M., Notredame, C., Huang, Q., et al. (2010). Long noncoding RNAs with enhancer-like function in human cells. Cell *143*, 46–58.

Paralkar, V.R., Taborda, C.C., Huang, P., Yao, Y., Kossenkov, A.V., Prasad, R., Luan, J., Davies, J.O.J., Hughes, J.R., Hardison, R.C., et al. (2016). Unlinking an lncRNA from Its Associated cis Element. Mol. Cell *62*, 104–110.

Ricciotti, E., and FitzGerald, G.A. (2011). Prostaglandins and inflammation. Arterioscler. Thromb. Vasc. Biol. *31*, 986–1000.

Rinn, J., and Guttman, M. (2014). RNA Function. RNA and dynamic nuclear organization. Science *345*, 1240–1241.

Sauvageau, M., Goff, L.A., Lodato, S., Bonev, B., Groff, A.F., Gerhardinger, C., Sanchez-Gomez, D.B., Hacisuleyman, E., Li, E., Spence, M., et al. (2013). Multiple knockout mouse models reveal lincRNAs are required for life and brain development. eLife *2*, e01749.

Stamatoyannopoulos, J.A., Snyder, M., Hardison, R., Ren, B., Gingeras, T., Gilbert, D.M., Groudine, M., Bender, M., Kaul, R., Canfield, T., et al.; Mouse ENCODE Consortium (2012). An encyclopedia of mouse DNA elements (Mouse ENCODE). Genome Biol. *13*, 418.

Sunwoo, J.-S., Lee, S.-T., Im, W., Lee, M., Byun, J.-I., Jung, K.-H., Park, K.-I., Jung, K.-Y., Lee, S.K., Chu, K., and Kim, M. (2017). Altered Expression of the Long Noncoding RNA NEAT1 in Huntington's Disease. Mol. Neurobiol. *54*, 1577–1586.

Tong, Q., Gong, A.-Y., Zhang, X.-T., Lin, C., Ma, S., Chen, J., Hu, G., and Chen, X.-M. (2016). LincRNA-Cox2 modulates TNF-α-induced transcription of Il12b gene in intestinal epithelial cells through regulation of Mi-2/NuRD-mediated epigenetic histone modifications. FASEB J. *30*, 1187–1197.

Visel, A., Blow, M.J., Li, Z., Zhang, T., Akiyama, J.A., Holt, A., Plajzer-Frick, I., Shoukry, M., Wright, C., Chen, F., et al. (2009). ChIP-seq accurately predicts tissue-specific activity of enhancers. Nature *457*, 854–858.

Wang, D., Patel, V.V., Ricciotti, E., Zhou, R., Levin, M.D., Gao, E., Yu, Z., Ferrari, V.A., Lu, M.M., Xu, J., et al. (2009). Cardiomyocyte cyclooxygenase-2 influences cardiac rhythm and function. Proc. Natl. Acad. Sci. USA *106*, 7548–7552.

Wang, P., Xue, Y., Han, Y., Lin, L., Wu, C., Xu, S., Jiang, Z., Xu, J., Liu, Q., and Cao, X. (2014). The STAT3-binding long noncoding RNA lnc-DC controls human dendritic cell differentiation. Science *344*, 310–313.

Wang, P., Xu, J., Wang, Y., and Cao, X. (2017). An interferon-independent lncRNA promotes viral replication by modulating cellular metabolism. Science *358*, eaao0409.

Xue, Z., Zhang, Z., Liu, H., Li, W., Guo, X., Zhang, Z., Liu, Y., Jia, L., Li, Y., Ren, Y., et al. (2018). lincRNA-Cox2 regulates NLRP3 inflammasome and autophagy mediated neuroinflammation. Cell Death Differ. *39*, 432.

Yin, Y., Yan, P., Lu, J., Song, G., Zhu, Y., Li, Z., Zhao, Y., Shen, B., Huang, X., Zhu, H., et al. (2015). Opposing Roles for the lncRNA Haunt and Its Genomic Locus in Regulating HOXA Gene Activation during Embryonic Stem Cell Differentiation. Cell Stem Cell *16*, 504–516.

Yu, Z., Crichton, I., Tang, S.Y., Hui, Y., Ricciotti, E., Levin, M.D., Lawson, J.A., Puré, E., and FitzGerald, G.A. (2012). Disruption of the 5-lipoxygenase pathway attenuates atherogenesis consequent to COX-2 deletion in mice. Proc. Natl. Acad. Sci. U.S.A *109*, 6727–6732.

STAR★METHODS

KEY RESOURCES TABLE

REAGENT or RESOURCE	SOURCE	IDENTIFIER
Antibodies		
COX-2 (mouse) Polyclonal Antibody (aa 570-598)	CaymanChem	RRID:AB_160106
Bacterial and Virus Strains		
J2 virus		https://www.ncbi.nlm.nih.gov/pubmed/2695237
Lentivirus	Generated using plasmids from Addgene	Packaging plasmids
		12260 (psPAX2)
		12259 pMD2
Chemicals, Peptides, and Recombinant Proteins		
Lipopolysaccharide E.coli, Strain 0111:B4-Tlr4 ligand	InvivoGen	Tlrl-3pelps
Lipopolysaccharide E.coli 0111:B4	Sigma-Aldrich	L2630
Pam_3CSK_4	InvivoGen	Tlrl-pms
R848	InvivoGen	Tlrl-r848
Critical Commercial Assays		
ELISA kit mouse Il-6	R&D	DY406
ELISA kit mouse Ccl5 (RANTES)	R&D	DY478
ELISA kit mouse Chi31	BosterBio	EK0975
ELISA kit mouse Cxcl10/IP-10	R&D	DY466
Illumina Truseq stranded RNA library kit	Illumina	20020596
NEXTflex Rapid Illumina RNA-Seq Library Prep Kit	Bioo Scientific	5138-07
Deposited Data		
Basal Lung RNA-Sequencing of Wild-Type and *lincRNA-Cox2* KO mice	This paper	GSE117379
LPS Stimulated Lung and Spleen RNA-Sequencing of wildtype and *lincRNA-Cox2* KO mice	This paper	GSE117379
WT (MOLF) x *lincRNA-Cox2* KO (C57/Bl6) *lincRNA-Cox2* RNA-Sequencing	This paper	GSE117379
Experimental Models: Cell Lines		
L929 cells	ATCC	C3H/An, CCL-1
HEK293T cells	ATCC	CRL-3216
J2 virus expressing cells	Dr. Doug Golenbock UMASS Medical School	
Immortalized wildtype BMDM	This paper	
Immortalized Cas9 BMDM	This paper	
Immortalized *LincRNA-Cox2* KO BMDM	This paper	
Immortalized BMDM Cas9 KO *LincRNA-Cox2*	This paper	
Immortalized BMDM *LincRNA-Cox2* Mutant (intronless)	This paper	
Immortalized BMDM Cas9 Exon2 KO *LincRNA-Cox2*	This paper	
Immortalized BMDM CRISPRi Clone 1	This paper	
Immortalized BMDM CRISPRi Clone 2	This paper	
Experimental Models: Organisms/Strains		
LincRNA-Cox2 KO mice (C57Bl6)	Sauvageau et al., 2013	eLife
Wild-type mice (C57Bl6)	Sauvageau et al., 2013	eLife
Ptgs2 (Cox)-2 f/f mice	Yu et al., 2012	PNAS
Ptgs2 (Cox)-2 f/f x VaviCre mice	This paper	
LincRNA-Cox2 intronless mutant mice (C57Bl6)	This paper	
Wild-Type (MOLF) x *lincRNA-Cox2* KO (C57Bl6) mice	This paper	

(*Continued on next page*)

Continued

REAGENT or RESOURCE	SOURCE	IDENTIFIER
Oligonucleotides		
Ptgs2 F	CCTGGTCTGATGATGTATGC	
Ptgs2 R	GAGTATGAGTCTGCTGGTTTG	
Ptgs2 flox F	GCTGTGGGGCAGGAAGTC	
Ptgs2 flox R	TTGGAATAGTTGCTCATCACC	
LincRNA-Cox2 F	AAGGAAGCTTGGCGTTGTGA	
LincRNA-Cox2 R	GAGAGGTGAGGAGTCTTATG	
Il-6 F	AACGATGATGCACTTGCAGA	
Il-6 R	GAGCATTGGAAATTGGGGTA	
Ifi202b F	GGCAATGTCCAACCGTAACT	
Ifi202b R	TAGGTCCAGGAGAGGCTTGA	
LacZ F	GGAGTGCGATATTCCTGAGG	
LacZ R	CGCATCGTAACCGTGCATC	
Neat1 F	TTGGGACAGTGGACGTGTGG	
Neat1 R	TCAAGTGCCAGCAGACAGCA	
Actin F	TTGAACATGGCATTGTTACCA	
Actin R	TGGCATAGAGGTCTTTACGGA	
GapDH F	CCAATGTGTCCGTCGTGGATC	
GapDH R	GTTGAAGTCGCAGGAGACAAC	
LincRNA-Cox2 genotyping WT1 F	CTTATTTAGGAGGGTGGGAAGTC	
LincRNA-Cox2 genotyping WT R1	GTGGTGGAGCTAGTGTCTCTTAG	
LincRNA-Cox2 genotyping KO1 F	GGAGTGCGATCTTCCTGAGG	
LincRNA-Cox2 genotyping KO1 R	CGCATCGTAACCGTGCATC	
LincRNA-Cox2 genotyping Mutant F	GATGGCTGGATTCCTTTGAA	
LincRNA-Cox2 genotyping Mutant R	ATGCCCAGAGACAAAAAGGA	
LincRNA-Cox2 genotyping Exon2 F	TAGCGAGAGGGCTATGGACA	
LincRNA-Cox2 genotyping Exon2 R	GATGGCTGGATTCCTTTGAA	
gRNA_Cas9_Mutant_*lincRNA-Cox2*_dnstrm_g1	CATTTATTATCTCCCTTTGC	
gRNA_Cas9_Mutant_*lincRNA-Cox2*_dnstrm_g2	TACAGCATGTCTCCTGCAAA	
gRNA_Cas9_Mutant_*lincRNA-Cox2*_upstrm_g1	CTGTCAGATGTATCTTATTT	
gRNA_Cas9_Mutant_*lincRNA-Cox2*_upstrm_g2	GCTTGGCGTTGTGAAAAAGC	
gRNA_Cas9_Ctl (non-targeting)	GTCCATACGCATAATCACCG	
gRNA_Cas9_*lincRNA-Cox2*_KO_dnstrm_g1	ATCATTAACCTGTTATCATA	
gRNA_Cas9_*lincRNA-Cox2*_KO_dnstrm_g2	CTTCAATAGACATATCTTTA	
gRNA_Cas9_*lincRNA-Cox2*_KO_upstrm_g1	TCTTTGATGCAAGGAACTAC	
gRNA_Cas9_*lincRNA-Cox2*_KO_upstrm_g2	TTACACTGTTTATCGCTGGT	
gRNA_Cas9_*lincRNA-Cox2*_KO_Exon2_Upstream_g1	CATTTATTATCTCCCTTTGC	
gRNA_Cas9_*lincRNA-Cox2*_Exon2_Upstream_g2	TACAGCATGTCTCCTGCAAA	
gRNA_Cas9_*lincRNA-Cox2*_Exon2_Downstream_g1	ATCATTAACCTGTTATCATATGG	
gRNA_CRISPRi_NT (Nontargeting)	CCTACACGACGAACGCAGGT	
CRISPRi_*lincRNA-Cox2*_gRNA1	GTCCCGCGCATGATCTTGGA	
CRISPRi_*lincRNA-Cox2*_gRNA2	TCTTGGAGGCAAACGCAGAG	
CRISPRi_*Ptgs2*_gRNA1	AGTCAGGACTCTGCTCACGA	
CRISPRi_*Ptgs2*_gRNA2	TCGTGAGCAGAGTCCTGACT	
MOLF_Ptgs2lastexon_fwd	gaaCCAcctTGTTGGACAGGAGAGAAGGAAATGGC	
MOLF_Ptgs2lastexon_rev	CCAGCTTAGCCGCCTTTTGATTAGTACTGTAGGG	
Illumina_MOLF_Fwd-index1	aatgatacggcgaccaccgagatctacacgatcggaagagcacacgtctgaactccagtcacCTTGTA gcacaaaaggaaactcaccct	

(*Continued on next page*)

Continued		
REAGENT or RESOURCE	SOURCE	IDENTIFIER
Illumina_MOLF_Fwd-index2	aatgatacggcgaccaccgagatctacacgatcggaagagcacacgtctgaactccagtcacGCCAAT gcacaaaaggaaactcaccct	
Illumina_MOLF_Fwd-index3	aatgatacggcgaccaccgagatctacacgatcggaagagcacacgtctgaactccagtcacAGTTCC gcacaaaaggaaactcaccct	
Illumina_MOLF_Fwd-index4	aatgatacggcgaccaccgagatctacacgatcggaagagcacacgtctgaactccagtcacTAGCTT gcacaaaaggaaactcaccct	
Illumina_MOLF_Rev	CAAGCAGAAGACGGCATACGAGATCGACTCGGTGCCACTTTTTC	
Recombinant DNA		
pSICO empty vector zeocin	This paper	
pSICO *lincRNA-Cox2* vector zeocin	This paper	
pSICO lentiviral vector	Covarrubias et al., 2017	
Software and Algorithms		
GraphPad Prism V8	GraphPad	
Office for Mac	Microsoft	
Illustrator CS6	Adobe	
Bowtie	Adobe	http://bowtie-bio.sourceforge.net/bowtie2/index.shtml
Samtools	Li et al., 2009	http://samtools.sourceforge.net/
DeSeq2	Love et al., 2014	

CONTACT FOR RESOURCE AND SHARING

Further information and requests for resources and reagents should be directed to and will be fulfilled by the lead Contact, Susan Carpenter (sucarpen@ucsc.edu).

EXPERIMENTAL MODEL AND SUBJECT DETAILS

Maintenance of mice

UMass Medical School, UCSC and the Institutional Animal Care and Use Committee maintained mice under specific pathogen-free conditions in the animal facilities of University of Massachusetts Medical School and University of California Santa Cruz (UCSC) in accordance with the guidelines.

LincRNA-Cox2 KO mice

LincRNA-Cox2 deficient mice were generated as previously published (Sauvageau et al., 2013). Briefly, the entire *lincRNA-Cox2* locus was deleted (deletion size 5.9 kB, targeting vector coordinates in mm9 coordinates: chr1:152006173-152012078) using VelociGene technology and replaced with a lacZ reporter cassette, enabling reporter gene expression under the endogenous *lincRNA-Cox2* promoter. Initially, the targeting constructs were electroporated into VGF1 hybrid mouse embryonic stem (ES) cells, derived from a 129S6S v/Ev female to a C57BL/6 male. Speed congenics were performed at Jackson laboratory to obtain a fully backcrossed (99%) C57/BL6 *lincRNA-Cox2* line.

Ptgs2 (Cox2) f/f VavCre mice

For the generation of conditional *Ptgs2* deficient BMDMs, floxed *Ptgs2* mice which were generated on a C57/B6 and 129SV chimeric background (Wang et al., 2009) were crossed to mice expressing VavCre, thereby generating mice lacking *Ptgs2* expression in all hematopoietic cells. Successful deletion of exons 6,7 and 8 of *Ptgs2* was confirmed by genomic PCR, Western Blot and RT-qPCR using the primers published previously (Anderson et al., 2015).

CRISPR/Cas9-mediated generation of LincRNA-Cox2 intron-less mice

The guide RNA sequences targeting upstream and downstream of the intron of lincRNA-Cox2 are tabulated below. Guides were cloned using the same approach as described earlier. Once sgRNAs were confirmed by sequencing they were intro transcribed by inserting a T7 ahead of the guide sequence and using the megashortscript T7 kit from Ambion. The sgRNAs are purified using MEGAclear Transcription Clean-Up Kit (ThermoFisher) and eluted in elution buffer, followed by an additional ammonium acetate precipitation to concentrate the RNA. The concentrated sgRNA is re-suspended in nuclease-free water and prepared at a concentration approximate to 2 ug/ul. To prepare Cas9 we obtained the vector from Addgene 42229. We used this as a template for a PCR reaction

to insert T7 using the following primers F:TAATACGACTCACTATAGGGAGAATGGACTATAAGGACCACGAC, R: GCGAGCTCTAG GAATTCTTAC. The mRNA transcript was generated using mMESSAGE mMACHINE T7 ULTRA kit from Life Technologies according to the manufactorers protocol. Cas9 was used at a final concentration of 100ng/ul and the guides at 25ng/ul and were injected into the cytoplasm of fertilized oocytes at the injection facility at UCSF.

Cell culture and BMDM differentiation

Cells were cultured in D-MEM with 10% fetal bovine serum (FCS) supplemented with penicillin/streptomycin and ciprofloxacin. Primary BMDM were generated by cultivating erythrocyte-depleted bone marrow cells in the presence of 20% L929 supernatant and the cells were used for experiments 6-9 days after differentiation. J2Cre virus (Blasi et al., 1989) was used on day 3/4 after isolation of bone marrow cells to establish transformed BMDM cell lines. BMDMs were cultivated in the presence of J2Cre virus for 48h and L929 was then gradually tapered off over 6-10 weeks depending on the growth pattern of transformed cells.

METHOD DETAILS

LPS shock model

Age- and sex matched wild-type and mutant mice (8-12 weeks of age) were injected i.p. with 20 mg/kg LPS (E.coli). For gene expression analysis and cytokine analysis, mice were euthanized 6 h post injection. Blood was taken immediately post mortem by cardiac puncture. Serum was isolated and sent to Eve technologies for cytokine analysis. Statistics were performed using GraphPad prism.

In vitro stimulation of BMDMs

Bone marrow cells were stimulated with Toll-like receptor (Tlr) ligands for the indicated time points using the following concentrations: Lipopolysaccharide (LPS) 100ng/ml (Tlr4), Pam_3CSK_4 100ng/ml (Tlr1/2), Pam_2CSK_4 100ng/ml (Tlr2/6), Poly(I:C) 25 μg/ml (Tlr3), R848 1μg/ml (Tlr7/8). For RNA and protein isolation, 1-2x10^6 cells were seeded in a 12-well format, for cytokine measurement 1-2x10^5 cells were plated in 96-well plates. Normalization of cell number for ELISA experiments was performed by CellTiter Glo Analysis.

Transfection and stable lentiviral overexpression of lincRNA-Cox2

The sequence of *lincRNA-Cox2* (synonym: Ptgs2os2) has been previously published (Carpenter et al., 2013; Guttman et al., 2009). Stable lentiviral overexpression and trans-rescue was performed with a pMSCVneo retroviral vector containing the mature sequence of *lincRNA-Cox2* (Carpenter et al., 2013). For generation of self-inactivating retroviral particles, HEK293T cells were transfected with packaging vectors VSVg (1μg), Gag-Pol (1μg) and pMSCVneo-*lincRNA-Cox2* (3μg). Genejuice was used as a transfection reagent according to manufacturer's instructions. Transfection media was removed 5h after transfection. Viral supernatants were collected 48 and 72 hours after transfection, filtered and used for transduction of BMDMs. BMDMs were incubated with viral supernatants for 48 hours, and neomycin (100μg/ml) was used for selection of transduced cells. For electroporation of primary BMDMs, cells were harvested from the bone marrow of WT and lincRNA-Cox2 KO mice and differentiated using MCSF from L929 cells as previously described. On day 4 of differentiation cells were transfected with 2ug of *lincRNA-Cox2* (pSico-vector) or with a control pSico-vector using the Lonza AD electroporation BMDM kit (VPA1009) as per the manufacturer's description.

CRISPR/Cas9 mediated deletion of lincRNA-Cox2 in immortalized BMDMs

The Cas9 construct was constructed from a pSico lentiviral backbone with an EF1a promoter expressing T2A flanked genes: blastocidin resistant (blast), Blue Fluorescent Protein (BFP), and humanized *Streptococcus pyogenes* Cas9. The single guide RNA (sgRNA) construct was also constructed from a pSico lentiviral backbone driven by EF1a promoter expressing T2A flanked genes: puro and cherry. sgRNAs were expressed from a mouse U6 promoter. Cloning of 20nt sgRNA spacer forward/reverse oligos were annealed and cloned via the AarI site. Immortalized bone marrow derived BMDMs (iMacs) were lentivirally infected with the Cas9 construct and was selected using blasticidin (1ug/ml) for 7 days. Cells were then lentivirially infected with either nontargeting guide or the guides targeting *lincRNA-Cox2* and were selected using puromycin (2ug/ml) for 7 days. Control and *lincRNA-Cox2* targeted cells were cloned out. Knockout of *lincRNA-Cox2* was confirmed by RT-qPCR.

CRISPRi mediated KO of lincRNA-Cox2 and Ptgs2 in immortalized BMDMs

Similar to the Cas9 construct, our dCas9-krab plasmid was constructed from a pSico lentiviral backbone with an EF1a promoter expressing T2A flanked genes: blastocidin resistant (blast), Blue Fluorescent Protein (BFP), and humanized *Streptococcus pyogenes* dCas9. The single guide RNA (sgRNA) construct was the same as described in the previous section. Immortalized bone marrow derived BMDMs (iMacs) were lentivirally infected with the dCas9-krab (described above) construct and was selected using blasticidin (1ug/ml) for > 2 weeks to obtain dCas9-krab expressing cells. Cells were then lentivirially infected with either non-targeting guide or gene targeted guide RNAs and were selected using puromycin (2ug/ml) for 7-14 days. Knockdown of *lincRNA-Cox2* or *Ptgs2* was confirmed by qRT-PCR.

RNA isolation and cDNA synthesis and RT-qPCR

Total cellular RNA from BMDM cell lines or tissues was isolated using the Direct-zol RNA MiniPrep Kit (Zymo Research) according to manufacturer's instructions. For tissue, RNA was isolated with the TRIZOL method after tissue homogenization. RNA was quantified and controlled for purity with a nanodrop spectrometer. (Thermo Fisher). For RT-qPCR, 500-1000 ng were reversely transcribed (iScript Reverse Transcription Supermix, Biorad) followed by RT-PCR (iQ SYBRgreen Supermix, Biorad) using the cycling conditions as follows: 50°C for 2 min, 95°C for 2 min followed by 40 cycles of 95°C for 15 s, 60°C for 30 s and 72°C for 45 s. The melting curve was graphically analyzed to control for nonspecific amplification reactions.

RNA-Sequencing

For generation of RNA-Sequencing libraries, RNA was isolated as described above and the RNA integrity was tested with a BioAnalyzer (Agilent Technologies) or FragmentAnalyzer (Advanced Analytical). For RNA-Sequencing target RIN score of input RNA (500-1000ng) usually had a minimum RIN score of 8. RNA-Sequencing libraries were prepared with TruSeq stranded RNA sample preparation kits (Illumina), depletion of ribosomal RNA was performed by positive selection of polyA+ RNA. Sequencing was performed on Illumina HighSeq or NextSeq machines. RNA-seq 50bp reads were aligned to the mouse genome (assembly GRCm38/mm10) using TopHat. The Gencode M13 gtf was used as the input annotation. Differential gene expression specific analyses were conducted with the DESeq R package. Specifically, DESeq was used to normalize gene counts, calculate fold change in gene expression, estimate p values and adjusted p values for change in gene expression values, and to perform a variance stabilized transformation on read counts to make them amenable to plotting. Data was submitted to GEO GSE117379.

MiSeq

For the MOLF experiment, 5ul of cDNA from MOLF-WT or MOLF-KO (2 mice each) was used to template a PCR reaction using 1uM of primers: Ptgs2lastexon_fwd: gaaCCAcctTGTTGGACAGGAGAGAAGGAAATGGC and Ptgs2lastexon_rev: CCAGCTTAGCCGCCT TTTGATTAGTACTGTAGGG and using the following cycle parameters: 1x (98C for 30 s), 20x (98C for 15 s, 56C for 15 s, 72C for 30 s) and 1x (72C for 10 min) using phusion 2X master mix (ThermoFisher, F0531). PCR products (MOLF-WT, MOLF-WT, MOLF-KO, MOLF-KO) were purified using Macherey-Nagel Gel-extraction columns, were digested with BstXI/Blp and were ligated into pU6-sgRNA vector (https://benchling.com/s/CXQ8OiQn/edit) (gift from the Weissman Lab, UCSF) using standard T4 ligase. Ligation was transformed, and coverage was determined to be > 200 colonies for each ligation. Using 1ul of the ligation reaction, we template a second PCR reaction using 1uM of the custom illumina primers (Liu et al., 2017).

Using the following cycle parameters: 1x (98C for 30 s), 20x (98C for 15 s, 56C for 15 s, 72C for 30 s) and 1x (72C for 10 min). PCR products were gel extracted on a 1% agarose gel and were purified using Macherey-Nagel Gel-extraction columns. Amplicons were sequenced on the MiSeq using the custom sequencing. For each sample, counts were generated for MOLF or C57/Bl6 *Ptgs2* alleles respectably using sequences: and were normalized to total reads for analysis. Data was submitted to GEO GSE117379.

Measurement of prostaglandins by mass spectrometry

Prostaglandin E2 production was measured by liquid chromatography/mass spectrometry as previously described [16]. Briefly supernatants were collected from Wild-Type or KO BMDMs following LPS stimulation for 6h. Systemic production of PGE_2, determined by quantifying the major urinary metabolites 7-hydroxy-5, 11-diketotetranorprostane-1, 16-dioic acid (PGEM). Results were normalized with creatinine.

Western Blot Analysis

For western blotting, BMDMs were scraped, washed and lysed buffer containing 20mM Tris-HCl (pH 7.4), 1% NP-40 and 5mM EDTA supplemented with Protease inhibitor (Promega). Clarified samples were separated by SDS-PAGE and transferred to PVDF membranes using the Trans-Blot® Turbo Transfer System (BioRad). After blocking of the PVDF membrane with PBS containing 5% (w/v) skim-milk powder and 0.1% Tween-20, the blots were probed with anti-COX2 (Cayman Item #160106) or anti-Actin (Sigma) antibodies. Visualization was performed with enhanced chemiluminescence substrate (ECL Pierce).

LacZ staining

For detection of reporter gene expression in *lincRNA-Cox2* deficient mice, selected tissue was dissected and fixed in 4% paraformaldehyde (PBS) for 5 hours (4°C). Fixed tissues were washed 3x with wash buffer (2mM $MgCl_2$, 0,01%sodium deoxycholate, 0,02% NP-40) and subsequently incubated in staining buffer (1mg/ml X-Gal, 5mM potassium ferricyanide, 5mM potassium ferrocyanide, 2mM $MgCl_2$, 0.01% sodium deoxycholate, 0.02% NP-40) in the dark overnight (room temperature). Staining solution was rinsed off with PBS 3x and tissue were frozen in OCT on dry ice and sectioned in 10μm sections.

QUANTIFICATION AND STATISTICAL ANALYSIS

For *in vivo* studies

All *in vivo* studies were carried out using $n \geq 5$. In every figure, each dot represents an individual animal. Student's t tests were performed using GraphPad Prism7. Asterisks indicate statistically significant differences between mouse lines (* = > 0.05, ** = > 0.01 and *** = > 0.005).

For *in vitro* studies

Data represents 3 combined biological replicates, representative of 3 individual experiments. Student's t tests were performed using GraphPad Prism7. Asterisks indicate statistically significant differences between mouse lines (* = > 0.05, ** = > 0.01 and *** = > 0.005).

DATA AVAILABILITY

All sequencing data generated from Mi-Seq and RNA-seq reported in this paper have been deposited to GEO under the ID code GSE117379.